ARTIFICIAL INTELLIGENCE BASED SPATIOTEMPORAL ENSEMBLE MODELING FOR MULTI-STATION PREDICTION OF PRECIPITATION

A THESIS SUBMITTED TO THE GRADUATE SCHOOL OF APPLIED SCIENCES OF NEAR EAST UNIVERSITY

By
SELİN ÜZELALTINBULAT

In Partial Fulfilment of the Requirements for the Degree of Doctor of Philosophy in COMPUTER ENGINEERING

NICOSIA, 2019

SELİN ÜZELALTINBULAT
ARTIFICIAL INTELLIGENCE BASED SPATIOTEMPORAL ENSEMBLE MODELING FOR MULTI-STATION PREDICTION OF PRECIPITATION
NEU 2019

ARTIFICIAL INTELLIGENCE BASED SPATIOTEMPORAL ENSEMBLE MODELING FOR MULTI-STATION PREDICTION OF PRECIPITATION

A THESIS SUBMITTED TO THE GRADUATE SCHOOL OF APPLIED SCIENCES OF NEAR EAST UNIVERSITY

By
SELİN ÜZELALTINBULAT

In Partial Fulfilment of the Requirements for the Degree of Doctor of Philosophy in Computer Engineering

NICOSIA, 2019

I hereby declare that all information is this document has been obtained and presented in accordance with academic rules and ethical conduct. I also declare that, as required by these rules and conduct, I have fully cited and referenced all material and results that are not original to this work.

Selin Üzelaltınbulat

Signature:

Date:

ACKNOWLEGMENT

In the beginning, would like to express my special appreciation and thanks to my advisors Professor Dr. Fahreddin Sadıkoğlu and Prof. Dr. Vahid Nourani, they have been a tremendous mentor for me and guide me well throughout the research work from topic's selection to finding the results. Their immense knowledge, motivation and patience have given me more power and spirit to excel in the research writing. Conducting the academic study regarding such a difficult topic couldn't be as simple as he made this for me. They are my mentor and a better advisor for my doctorate study beyond the imagination. They all have played a major role in polishing my research writing skills.

Also Prof. Dr. Rahib Abiyev supported me well throughout the entire research program. Him immense support actually guided me to rectify numerous things that could create major challenges in my PhD process.

And I would like to thanks to Assist. Prof. Dr. Boran Şekeroğlu for him support, patience, good intentions and great friendship.

Apart from my Supervisors, I won't forget to express the gratitude to rest of the people. Thank you Dr. Gholamreza Andalib and Nazanin Behfar for giving the encouragement and sharing insightful suggestions. It wouldn't have been possible to conduct this research without their precious support. They all really mean a lot to me.

In the end, I am grateful to my family who remembered me in their prayers for the ultimate success. They gave me enough moral support, encouragement and motivation to accomplish the personal goals. Their prayer for me was what sustained me thus far. I would also like to say a heartfelt thank you to darling Emre for always believing in me and encouraging me to follow my dreams and for helping in whatever way they could during this challenging period.

Finally, I thank my God, for letting me through all the difficulties. I have experienced. You are the one who let me finish my degree. I will keep on trusting you for my future.

ABSTRACT

Precipitation is the most important environmental, natural and climatic process all around the world and its accurate prediction plays a crucial role in hydro-environmental studies. Precipitation has negative and positive impacts on the agriculture, economy, tourism, ecosystem, water resources management etc. However, because of the non-linearity, irregularity and uncertainty of precipitation, the prediction of precipitation is a quite difficult task. The current literature for prediction of precipitation is commonly used Artificial Intelligence (AI) based single models such as Feed Forward Neural Network (FFNN), Adaptive Neuro-Fuzzy Inference System (ANFIS) and Least Square Support Vector Machine (LSSVM) . AI-based on single models do not provide required precision in prediction of precipitation.

To increase the precision of prediction using AI-based models, the author proposes temporal-spatial ensemble modeling allows to increase the precision and predict the precipitation in the whole geographical area.

Application of ensemble techniques based on nonlinear averaging of the outputs of AI-based single models allows to increasing precision of prediction of precipitation. The linkage of the temporal modeling with spatial modeling based on Inverse Distance Weight (IDW) interpolation allows to predicting the precipitation in the whole geographical region.

For simulation and computation were used 10 years' monthly data from seven metrological stations located in different regions of the Turkish Republic of Northern Cyprus (TRNC). Numerical simulations of proposed spatio-temporal modeling and analysis of the results show the validity of proposed models for efficient prediction of precipitation in TRNC.

Keywords: Precipitation; artificial intelligence; ensemble method; spatio-temporal modeling; inverse distance weighting

ÖZET

Yağış, tüm dünyada en önemli çevresel, doğal ve iklimsel olaydır ve hidro-çevresel çalışmaların doğru tahmin edilmesinde önemli rol oynar. Yağış, tarım, ekonomi, turizm, ekosistem, su kaynakları yönetimi gibi konular üzerinde olumsuz ve olumlu etkilere sahiptir. Ancak, yağışların doğrusal olmaması, düzensizliği ve belirsizliği nedeniyle, yağış tahmini oldukça zor bir iştir. Yağış tahmini için güncel literatürde, İleri Besleme Sinir Ağı (FFNN), Uyarlanabilir Nöro-Bulanık Çıkarım Sistemi (ANFIS) ve En Küçük Kare Destek Vektör Makinesi (LSSVM) gibi Yapay Zeka (AI) tabanlı tekli modeller kullanılmıştır. AI tabanlı tekli modeller yağış tahmininde gerekli hassasiyeti sağlayamamaktadır.

Yazar, AI tabanlı modellemede tahmin hassasiyetini artırmak için topluluk yöntemini ve tüm coğrafi alandaki yağışların tahmini için ise zamansal-mekansal modelleme önerisini sunmaktadır.

AI tabanlı tekli modellerin çıktılarının doğrusal olmayan ortalamalarına dayanan topluluk tekniklerinin uygulanması, yağış tahmininin kesinliğini arttırmaya izin verir. Zamansal modellemenin Ters Mesafe Ağırlığı (IDW) enterpolasyonuna dayanan mekansal modelleme ile bağlanması ise, tüm coğrafi bölgedeki yağışların tahmin edilmesine olanak sağlar.

Simülasyon ve hesaplama için, Kuzey Kıbrıs Türk Cumhuriyeti'nin (KKTC) farklı bölgelerinde yer alan, yedi metroloji istasyonundan 10 yıllık süreyi kapsayan aylık veriler kullanılmıştır. Sayısal simülasyonlar zamansal-mekansal modelleme ve sonuçların analizi, KKTC'de yağışların etkin bir şekilde tahmin edilmesi için önerilen modellerin geçerliliğini göstermektedir.

Anahtar Kelimeler: Yağış; yapay zeka; birleştirilmiş topluluk metodu; zamansal-mekansal modelleme; ters mesafe ağırlıklandırma

TABLE OF CONTENTS

LIST OF TABLES

LIST OF FIGURES

LIST OF ABBREVIATIONS

ACF:	Auto-correlation Function
AI:	Artificial Intelligence
ANFIS:	Adaptive Neural Fuzzy Inference System
ANN:	Artificial Neural Network
BP:	Back Propagation
CC:	Correlation Coefficient
DC:	Determination Coefficient
FIS:	Fuzzy Inference System
FFNN:	Feed Forward Neural Network
FFNN-BP:	Feed Forward Neural Network with Backpropagation
GPRS:	General Packet Radio Service
IDW:	Inverse Distance Weighting
LL:	Lower Limit
L-SVM:	Linear Support Vector Machine
LSSVM:	Least Square Support Vector Machine
MF:	Membership Function
MI:	Mutual Information
MLFF:	Multi-Layer Feed Forward
MLFFNN:	Multi-Layer Feed Forward Neural Network
NA:	Non-linear Averaging
N-SVM:	Non-linear Support Vector Machine

RBF: Radial Basis Function

RMSE: Root Mean Square Error

SS: Skill Score

SLA: Simple Linear Averaging

SVM: Support Vector Machine

TRNC: Turkish Republic of Northern Cyprus

TSK: Takagi-Sugeno Kang

WA: Weighted Averaging

UL: Upper Limit

LIST OF NOMENCLATURE

Symbol	Description
A:	Measure of accuracy
B:	Membership functions parameter B
b:	Bias
C:	Membership functions parameter C
e_i:	Slack variable
H(x):	Entropy of X
H(x,y):	Joint entropy of X and Y
N:	Number of single models
n:	Data number
P:	Outlet function variable
P_{obs}:	Monthly observed precipitation (mm/month)
P_{com}:	Monthly calculated precipitation (mm/month)
$P_{(max)t}$:	Max value of monthly observed precipitation (mm/month)
$P_{(min)t}$:	Min value of monthly observed precipitation (mm/month)
$P^i(t)$:	Precipitation of station at i time t (mm/month)
P(t-α):	Previous monthly precipitation value corresponding to α month ago (mm/month)
$P^{Ercan}(t)$:	Monthly precipitation of Ercan station at time t (mm/month)
P(t):	Precipitation monthly data (m/month)
q:	Outlet function variable q
r:	Outlet function variable r

t: Time (month)

w: Weight

α: Lagrange multiplier

γ: Margin parameter

λ: Kernel parameter

ϕ: Kernel function

CHAPTER 1
INTRODUCTION AND OVERVIEW

1.1 Background of the Problem

Precipitation is one the most important meteorological event on the earth and occurs when a portion of the atmosphere becomes saturated, so that the water condenses and precipitates (Alpers and Melsheimer, 2004).

Precipitation's cause-effect relationships cannot be expressed in simple or complex mathematical forms and it is considered the hardest weather variable to forecast. The phenomenon of precipitation have differences in latitude, longitude, regions, planes and mountainous (Alpers and Melsheimer, 2004).

Precipitation is the most important component of the hydrologic cycle and accurate modeling of precipitation. However, due to complex, non-linear and stochastic nature of precipitation over both time and space domins, its spatiotemporal modeling is quite a difficult task for the hydro-climatologists. For such a spatiotemporal modeling of hydro-climatologic processes, usually a time series prediction model is linked to a spatial interpolation tool (e.g. see, Rizzo and Dougherty, 1994; Nourani et al., 2010; Sahoo et al., 2017; Souto et al., 2018).

Once the accurate estimations for the process are more crucial than the physics interprations, utilizing data driven (black box) methods will be better alternatives to the physically based methods. Recently, Artificial Intelligence (AI) methods such as black box methods showed great efficiency in modeling the dynamic process in the presence of the non-linearity, uncertainty and irregularity of the used data. Comparative researches have shown that the AI-based models may generate reliable results of precipitation predictions with regard to the physically based models (Abbot and Marohasy, 2012).

One of the most commonly used AI methods for the precipitation modeling is ”Feed Forward Neural Network (FFNN)” which is a common type of Artificial Neural Network (ANN) methods.

As another type of AI model, one of the most effective predicting methods as an alternative method of ANN is the “Least Square Support Vector Machine (LSSVM).”

In addition to the ANN and LSSVM methods, the “Adaptive Neural Fuzzy Inference System (ANFIS)” model, which incorporates both the ANN learning power and fuzzy logic representation, has been considered as a robust model for precipitation prediction because of fuzzy concept ability in handling the uncertainty involved in the study processes.

The uncertainty associated with any predection indicates that different scenarios are possible and the predection must reflect all. By providing a range of possible outputs, the model shows how likely various scenarios come true in the months ahead, and which methods are useful and for how long they are useful in the future forecasts. In addition to the temporal modeling (time series prediction), spatial interpolator can be useful tools to estimate the precipitation for any desired point within the study region where there is not any installed rainfall gauge. Geostatistical methods have been extensively employed in hydro-climatic modeling to estimate the missing data points without observation instruments (e.g. see, Caruso and Quarta, 1998; Theodossiou and Latinopoulos, 2006; Nourani et al., 2010). Among several Geostatistical methods, Inverse Distance Weighting (IDW) method could gain the attention of the researchers due to its simpility and reliable accuracy (e.g. see, Chen and Liu, 2012; Shahidi and Abedini, 2018).

1.2 Literature Review

In the recent decades, FFNN has acquired increasing popularity due to its flexibility and robustness to detect involved patterns in the various range of data. For examples, Guhathakurta (2008) employed ANN for prediction of the monthly precipitation over 36 meteorological stations of India to estimate the monsoon precipitation of upcoming years. The model could catch nonlinear interactions among input and output data and estimate the seasonal rainfall. Hung et al. (2009) employed ANN for real time precipitation predicting and flood management in Bangkok, Thailand. It was found out that the most dominant inputs in modeling are rainfall values at previous time steps (as a Markovian process). Likewise, Abbot & Marohasy (2012) predicted monthly and seasonal precipitations up to 3 months in advance over Queensland, Australia, by using dynamic, recurrent and time-delay ANNs. More recently, Khalili et al. (2016) employed the Hurst rescaled range statistical analysis to evaluate the predictability of the available data for monthly precipitation prediction of Mashhad City, Iran. Devi et al. (2017) applied ANNs for forecasting the rainfall time series using the temporal and spatial rainfall intensity data and pointed to the wavelet-Elman model as the best method for rainfall forecasting. Mehdizadeh et al. (2018) introduced two novel hybrid models of ANN autoregressive conditional heteroscedasticity (ANN-ARCH) and gene expression programming-autoregressive conditional heteroscedasticity (GEP-ARCH) for forecasting monthly rainfall time series. They indicated that GEP-ARCH and ANN-ARCH methods could lead to reliable outcomes for the studied regions with different climatic conditions. They also revealed that ANN-ARCH method can present more reliable results with regard to the GEP-ARCH method.

In addition to the ANN, the Adaptive Neural Fuzzy Inference System (ANFIS) model, which merges the ANN learning power and fuzzy logic knowledge representation, has been considered as a robust model for precipitation prediction because of fuzzy concept ability in handling the uncertainty involved in the study processes. The ANFIS can analyse the relationship involved in the input and output data sets via a training scheme to optimize the parameters of a given Fuzzy Inference System (FIS) (Akrami et al. 2014). Some previous investigations indicated that ANFIS can be used as an efficient tool for precipitation modeling. For example, ANFIS and ANNs models were trained and tested for mentioned years and consequently the predictive results of models compared with the results of SCS method (Sharifi et al., 2013). The another study was carried out to develop rainfall forecasting model whish is ANFIS was used for developing models rainfall of Udaipur city. Statistical and hydrologic performance indices of ANFIS gave better performance among developed four models (Sojitra et al., 2015). Yaseen et al., (2018) employed a new hybrid model integrated ANFIS with Firefly Optimization algorithm (ANFIS-FFA) is proposed for forecasting monthly rainfall with one-month lead time. The proposed ANFIS-FFA model is compared with standard ANFIS model. Certainly that the ANFIS-FFA is a prudent modelling approach that could be adopted for the simulation of monthly rainfall in the present study region. Some previous investigations indicated that ANFIS can be used as an efficient tool for precipitation modelling Keskin et al., (2006) employed to develop a flow prediction method, based on the ANFIS coupled with stochastic hydrological models. An ANFIS methodology is applied to river flow prediction in Dim Stream in the southern part of Turkey. As a result, the extension of input and output data sets in the training stage improves the accuracy of forecasting by using ANFIS.

As another type of AI model, the Least Square Support Vector Machine (LSSVM) is one of the most effective predicting methods as an alternative method of ANN. The LSSVM is capable of predicting non-linear, non-stationary and stochastic processes (Granata et al. 2017). The LSSVM has been used for prediction of precipitation in the recent decades. Lu & Wang (2011) forecasted the monthly precipitation over a state in China employing LSSVM method using several kernel functions. Using the available observed data of 2 different stations from Turkey, Kisi & Cimen (2012) employed the LSSVM with and without wavelet based data pre-processing technique for prediction of precipitation time series. Sharifi et al. (2013) examined a large numbers of predictants for the pourpose of precipitation estimation and evaluated the contributions of the humidity and Equivalent Potential Temperature parameters in the Support Vector Machine (SVM) based precipitation modeling as a process which involves a high degree of uncertainty. More recently, Danandeh Mehr et al. (2018) developed a hybrid regression method on the basis of the”Support Vector Regression (SVR)”and”firefly algorithm (FFA) for precipitation predection of rain gauges with promising accuracy. The outcomes revealved that the proposed combined method can significantly outperform the single SVR and GEP methods. Also the recent decade highlighted the efficiency of wavelet-based LSSVM (WLSSVM) model was examined for prediction of daily and monthly Suspended Sediment Load of the Mississippi River. For this purpose, the ability of WLLSVM was compared with other models then the results show that LSSVM has better outcomes (Nourani and Andalib, 2015).

With the recent developments in the AI techniques, althgough ANN, ANFIS and LSSVM have been reliably employed to model time series of varios hydro-climatic variables (including precipitation), it is obvious that for a particular problem, different outcomes can be have from different models over different spans of the time series. As such, Bates & Granger (1969) suggested that, different ensemble approaches, compared to single techniques would provide the results with minimum error variance. Also, Makridakis et al. (1982) revealed improving the forecasting accuracy by combining the results from the single models. Yamashkin et al. (2018) confirmed that reliability, objectivity, and accuracy of the analysis are increased by the use of ensemble systems. Sharghi et al. (2018) indicated that performance of the seepage modeling can be enhanced by the ensemble method up to 20%. The ensemble precipitation prediction is a set of forecasts that presents the range of future rainfall possibilities with a minimized error. The uncertainty associated with any predection indicates that different scenarios are possible and the predection must reflect all. By providing a range of possible outputs, the model shows how likely various scenarios come true in the months ahead, and which methods are useful and for how long they are useful in the future forecasts.

Although the ensemble approaches have been focused during the last decades at different engineering fields (e.g., Kasiviswanathan et al., 2013; Zhang, 2003; Kourentzes et al., 2014), to the best knowledge of of the authors, this paper presents the first AI-based ensemble approach for precipitation modeling solely and also linked to a spatial interpolation.

In addition to the temporal modeling (time series prediction), spatial interpolators can be useful tools to estimate the precipitation for any desired point within the study region where there is not any installed rainfall gauge. Geostatistical methods have been extensively employed in hydro-climatic modeling to estimate the missing data or peroides at points without observation instruments (e.g. see, Caruso & Quarta 1998; Theodossiou & Latinopoulos 2006; Nourani et al. 2010). Among several Geostatistical methods, Inverse Distance Weighting (IDW) method could gain the attention of the researchers due to its simpility and reliable accuracy (e.g. see, Chen & Liu 2012; Shahidi & Abedini 2018).

The objective of the present paper is spatio-temporal modeling of precipitation extended on a case study with seven rain gauges located in the "Turkish Republic of Northern Cyprus (TRNC)". To attain this goal, firstly ensemble of outputs of 3 AI models is conducted for temporal prediction of precipitation time series for all stations. Three techniques of ensembling, which are “simple, weighted linear and non-linear neural averaging” are applied for this pourpose. Then in the spatial modeling stage, the outputs of AI-based ensemble technique as predicted precipitation values of stations (results of temporal modeling stage) are used as inputs for the spatial interpolation of precipitation by the IDW method over whole region. Although the ensemble approaches have been focused during the last decades at different engineering fields (e.g., Kasiviswanathan et al. 2013; Zhang 2003; Kourentzes et al. 2014), to the best knowledge of of the authors, this paper presents the first AI-based ensemble approach for precipitation modeling solely and also linked to a spatial interpolation.

1.3 Statement of the Problem

The AI-based modeling (ANN, ANFIS or LSSVM) have acquired increasing popularity in prediction the dynamic precipitation process in the presence of the noise, non-linearity, uncertainty and irregularity inherent of the input data. The AI-based models provide flexibility, robustness and possibilities to handle nonlinearity and uncertainty. For this reason, AI-based models may generate reliable results with regard to the physically based models.

However, the single AI-based models show that in different parts of the time series, some of the models led to overestimations and others down estimations. The different performances of different AI-models for different time series for same time series at different time spans stipulate a need to ensemble the results of different methods that are diverse and non-accurate. Application of ensemble techniques based on nonlinear averaging allows to enhance the overall precision of time series prediction.

Estimation of the precipitation over the whole geographical region in terms of the data obtained from the limited number of precipitation stations is the second problem in this research. This problem solved by the spatial interpolations of the predicted time series using the IDW method.

1.4 Objective of the Research

Objective of the thesis is to develop the high-performance temporal-spatial modeling of precipitation. To achieve this goal were developed:

- Temporal modelling of prediction of precipitation using three AI-based single models (ANN, ANFIS and LSSVM) with non-linear averaging of the outputs.
- Spatial modelling of prediction of precipitation based on IDW interpolation to predict precipitation over the whole region.

1.5 Originality of the Thesis

Temporal-spatial modeling of the precipitation based on the ensembling of the outputs of single AI-based models and its linkage with spatial modeling developed the first time. The novelty of the proposed temporal-spatial modeling proven by the publications of the results in the SCI-journal and main scientific results of the research were presented and discussed in international conference in front of well-known scientists.

1.6 Problem Solution

In this thesis, for spatiotemporal modeling of precipitation in TRNC, a two-stage hybrid modeling was provided. The aim of time-space estimations of monthly precipitation via a two-stage modeling framework ensemble precipitation prediction in this thesis was to achieve the best performance via artificial intelligence (AI) based modeling. In temporal modeling, as the first stage, ensemble AI based modeling was proposed for prediction of monthly precipitation with three different AI models (FFNN, ANFIS and LSSVM) for the seven stations located in the TRNC. The monthly data covering ten years' precipitation were used for the predictions.

In this way, two scenarios were examined each having specific inputs set. The scenario 1 was developed for predicting each station's precipitation through its own data at previous time steps while in scenario 2, the central station's data were imposed into the models, in addition to each station's data, as exogenous input.

At the temporal stage two scenarios were considered with different input variables that in scenario 1 each station's own pervious data was used for modeling while in scenario 2, the central station's (Ercan station) data were also employed in addition to each station's own data. The results of two employed scenarios indicated that scenario 2 had better performance and could enhance the modeling efficiency up to 58%, in the verification step because of employing the observed data from the Ercan station as exogenous input in simulating other stations' precipitation.

Thereafter, the ensemble methods were employed to increase the temporal modeling efficiency. The ensemble modeling was generated to improve the performance of the precipitation predictions. The outputs of neural ensemble method (as the best temporal modeling tool) were utilized in the spatial modeling stage. In this stage, through seven steps for all stations, one station's data were individually removed from the modeling process and then, its values were estimated by the predicted values from six other stations for the verification period.

To end this aim, two linear and one non-linear ensemble techniques were used and then the obtained outcomes were compared. In the second stage, for estimation of the spatial distribution of precipitation over whole region. The results of temporal modeling used as inputs for the Inverse Distance Weighting (IDW) spatial interpolator. The cross-validation finally applied to evaluate the overall accuracy of the proposed hybrid spatiotemporal modeling approach.

CHAPTER 2
STUDY AREA AND DATA GATHERING

2.1 Description of the Study Area

Cyprus is located at approximately 35° N and 33°E, at the east end of the Mediterranean Sea, and is ~224 km WSW to ENE, and ~97 km NNW–SSE with a land area of approximately 9250 km^2 was shown in Figure 2.1. The island has two mountain ranges – the Troodos Massif (maximum elevation 1951 m) in the southwest and the Pentadaktylos (Girne) range (maximum height 1000 m) along the northern coast, which give Cyprus high topographical variability (Price et al., 1999).

The climate of North Cyprus is typical Mediterranean with hot dry summers where the average temperature can reach up to 40° C. In cool winter months the lowest temperature tends to be around 10° C.

Data from seven main stations were used in this study to predict the precipitation was shown in Figure 2.1. these are;

1) Ercan International Airport; at this station, the summers are hot, arid, and clear and the winters are cold, windy, and mostly clear. Over the course of the year, the temperature typically varies from 4°C to 35°C and is rarely below 0°C or above 37°C.

2) Gazimağusa's climate is classified as warm and temperate. In winter, there is much more rainfall in Gazimağusa than in summer. The average temperature in Gazimağusa is 19.3 °C and the average rainfall is 407 mm.

3) The prevailing climate in Geçitkale is known as a local steppe climate. During the year, there is little rainfall in Geçitkale and the average annual temperature is 19.1°C.

4) Girne station's climate is warm and temperate and the average annual rainfall is 382 mm. The winters are rainier than the summers. In Girne, the average annual temperature is 19.6 °C. Precipitation has averages of 449 mm.

5) Güzelyurt has a local steppe climate. There is little rainfall throughout the year. In Güzelyurt, the average annual values of temperature and pressure are respectively 18.5 °C and 363 mm.

6) Lefkoşa has a hot semi-arid climate due to its low annual precipitation and annual temperature range. The city experiences long, hot, dry summers, and cool to mild winters, with most of the rainfall occurring in winter. The winter precipitation is occasionally accompanied by sleet and rarely by snow. The accumulation of snow is particularly rare (last events occurred in 1950, 1974, 1997 and 2015). There is occasionally light frost during the winter nights. The temperature reached 44.7°C on 2nd July 2017 in Lefkoşa.

7) Yeni Erenköy's climate is classified as warm and temperate. There is more rainfall in the winter than in the summer in Yeni Erenköy. The average temperature in Yeni Erenköy is 18.7 °C and about 520 mm of precipitation falls annually.

For training and validation of the models, the average monthly data were obtained from these seven meteorological stations for ten years, from January 1, 2007, to December 31, 2016. The characteristics of the stations and also the statistics of the data from stations are tabulated in Table 2.1.

(a) General map of the study area (https://www.cyprusisland.net/where-cyprus)

(b) Location of the stations (www.beyburt.com)

Figure 2.1: Situation and locations of the study area

The geographical characteristics of the stations and also the statistics of the data from stations are tabulated in Table 2.1

Table 2.1: The characteristics of stations and statistics of the precipitation data

Station	Altitude (m)	Longitude	Latitude	Max (mm)	Mean (mm)	Std. Dev. (mm)
Ercan	123 m	33° 29' 59.99" E	35° 09' 21.00" N	71.0	25.2	0.97
Gazimağusa	1.8 m	33° 56' 20.18" E	35° 07' 13.94" N	104.7	27.9	1.27
Geçitkale	44 m	33° 23' 15" E	34° 49' 30" N	70.0	27.0	1.12
Girne	0 m	33° 19' 2.24" E	35° 20' 10.82" N	142.0	38.4	1.95
Güzelyurt	65 m	32° 59' 36.17" E	35° 11' 55.28" N	100. 7	23.7	1
Lefkoşa	220 m	33° 21' 51.12" E	35° 10' 31.12" N	66.2	22.8	0.92
Yeni Erenköy	22 m	34° 11' 30" E	35° 31' 60" N	76.0	33.3	1.46

2.2 Selection the Potential Input Variables for the Model

Usually, as a conventional method, linear correlation coefficient (CC) is computed between potential inputs and output to select most dominant input variables for the AI methods such as FFNN (Partal and Cigizoglu, 2008). However, implementation of CC for dominant input selection has been already criticized (e.g., see, Nourani et al., 2014) since for modeling a nonlinear process by a non-linear approach like FFNN, it will be more feasible to employ a nonlinear criterion (e.g., Mutual Information (MI)) since in spite of a weak linear relation, strong non-linear relationships may be existing among input and output parameters. The MI value between random variables of X and Y can be written in the form of (Yang et al. 2000):

$$MI(A,B) = H(A) + H(B) - H(A,B) \tag{2.1}$$

where A and B are the probability distributions of X and Y and H(A) and H(B) show the entropies of A and B respectively, and H(A,B) is their joint entropy as:

$$H(A,B) = -\sum_{a\epsilon A} \sum_{b\epsilon B} p_{AB}(a,b) log p_{AB}(a,b) \tag{2.2}$$

The MI between the observed precipitation time series of all seven stations relative to each other were calculated and tabulated in Table 2.2. As it can be seen from Table 2.2, overall, Ercan's precipitation data are more non-linearly correlated with the precipitation time series of other stations, maybe due to its central position with regard to the others.

Table 2.2: The MI between the observed precipitation time series of stations

Station	Ercan	Gazimağusa	Geçitkale	Girne	Güzelyurt	Lefkoşa	Yeni Erenköy
Ercan	-	0.993	1.038	1.085	0.958	1.074	0.992
Gazimağusa	0.993	-	0.939	0.893	0.964	0.971	0.941
Geçitkale	1.038	0.939	-	0.868	0.908	0.974	0.925
Girne	1.085	0.893	0.868	-	0.911	0.949	0.876
Güzelyurt	0.958	0.964	0.908	0.911	-	0.983	0.947
Lefkoşa	1.074	0.971	0.974	0.949	0.983	-	0.967
YeniErenköy	0.992	0.941	0.925	0.876	0.947	0.967	-
Mean MI	**1.02**	**0.950**	**0.942**	**0.931**	**0.945**	**0.986**	**0.941**

For instance, the Auto-correlation Function (ACF) of Ercan and Lefkoşa precipitation time series are presented in Figure 2.2. As it can be seen from Figure 2.2, the precipitation time series of some stations such as Ercan station are more auto-correlated with 1 and 12-month lags, whereas the precipitation time series of some other stations such as Lefkoşa station are more auto-correlated with 1, 2 and 12-month lags. As noticed previously, CC is unable to recognize the non-linear relation between time series. Therefore, in continue, the MI was employed to determine the non-linear relation between precipitation time series and their lag times. So, it was recognized that the precipitation time series are mostly correlated non-linearly with 1 and 12 month lags in all stations which denotes to both auto-regressive (Markovian) and seasonality of the process.

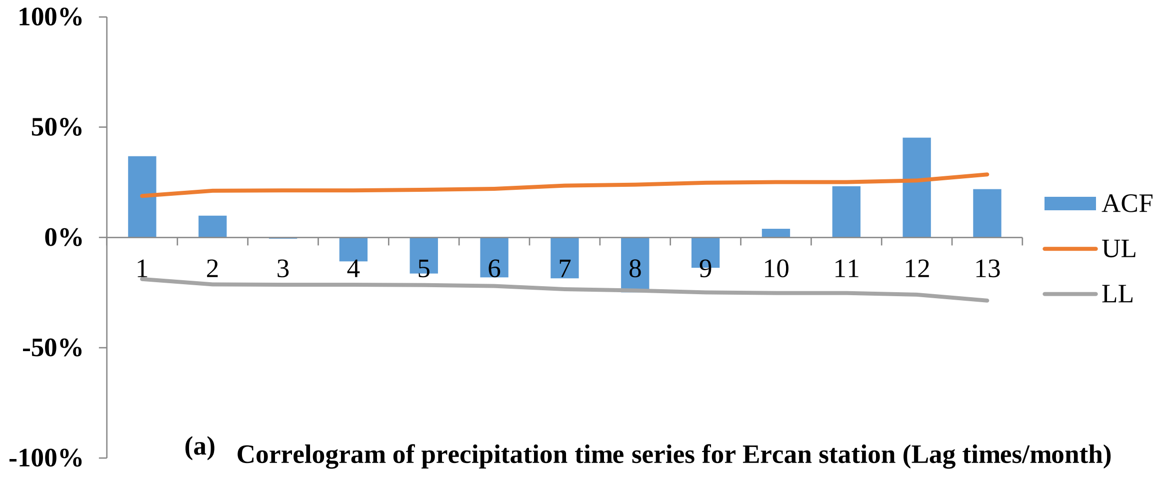

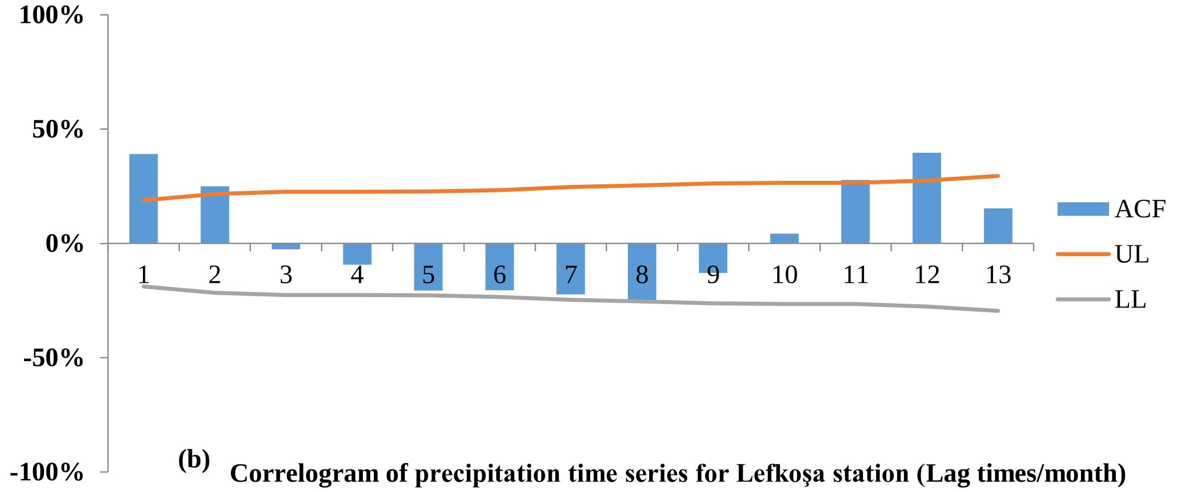

Figure 2.2: Correlogram of precipitation time series for (a) Ercan station, (b) Lefkoşa station; UL = Upper Limit; LL = Lower Limit.

Beside computing auto-correlation function, for testing the normality of data, Kolmogorov Smirnov test (Steinskog et al., 2007) was used and results indicated that the data of all 7 stations are non-normal; so nonparametric tests should be applied to these datasets. Next, the Run test (Adeloye and Montaseri, 2002; Vaheddoost and Aksoy, 2017) was employed for testing randomness of precipitation time series of each station. Results of Run test at 95%

confidence level indicated that precipitation of all stations are not random so that the precipitation of all stations are predictable. Also to check data homogeneity, Pettitt's test (Pettitt, 1979), Standard normal homogeneity test (SNHT) (Alexandersson, 1986), Buishand's test (Buishand, 1982) and Chi-square test (Moore, 1987) were applied to data of all stations which probed that data of stations are homogenous.

2.3 Data Gathering

2.3.1 Rain Gauge

It should be mentioned that automatic sensors are usually used to measure the precipitation data in TRNC which work with solar energy and battery system and precipitation is loaded into the data loggers and then data is collected with GPRS in every 15 minutes. Also the fine adjustment and calibration of the sensors are handled based on the international standards. The sensors' accuracy and sensitivity are ±2% and 0.2 mm, respectively. Figure 2.3 shows the situation of rain gauge with the installation equipment. Figure 2.4 shows the types of rain gauges which are used in this research. Also specifications of the rain gauges are tabulated in Table 2.3 and 2.4.

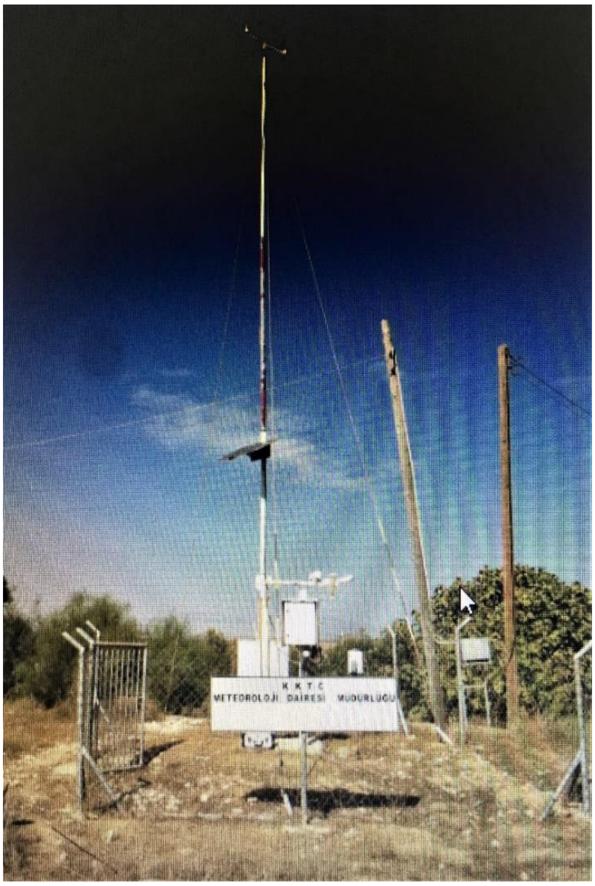

a)

b)

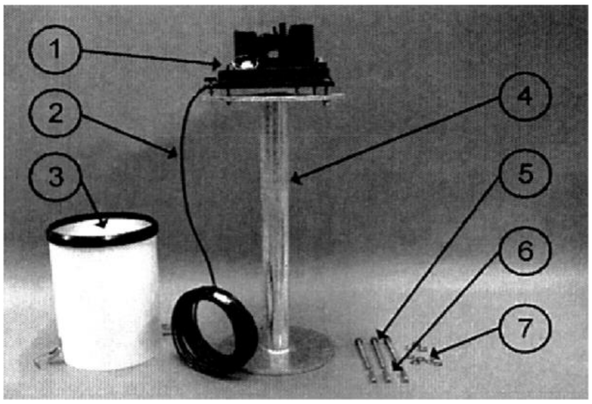

c)

Figure 2.3: a) Lefkoşa rain gauge station, b) Rain gauge solar energy and battery system c) Rain gauge with the installation equipment; 1 = Sensor base; 2 = Sensor cable; 3 = Outer tube; 4 = Stand; 5 = Mounting bolts for the stand; 6 = Wedge bolts; 7 = Nut and washers for mounting bolts.

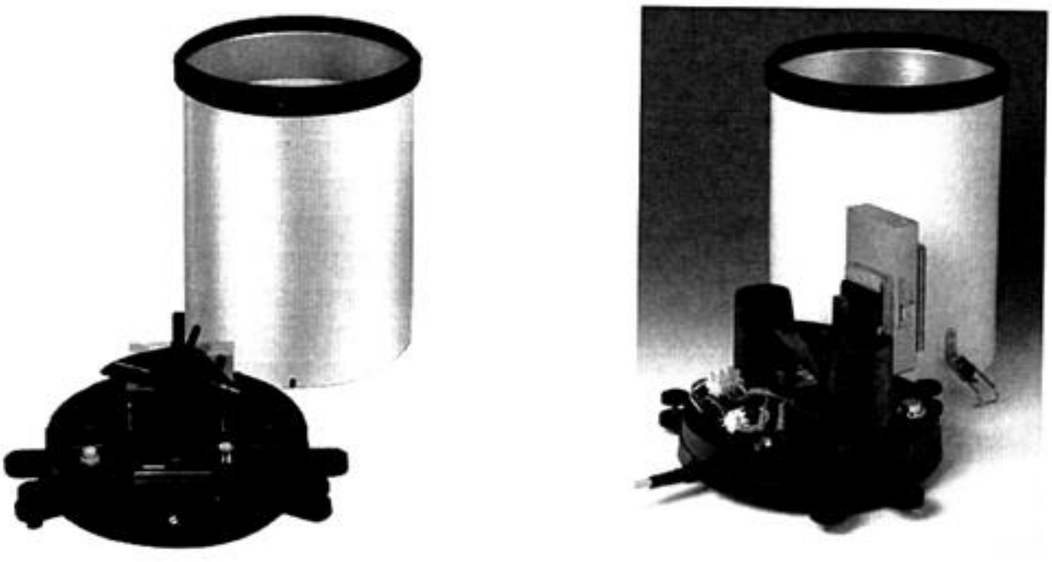

a) Rain gauge RG13 b) Heated Rain Gauge RG13H

Figure 2.4: Types of rain gauges

Table 2.3: Specifications of rain gauge RG13

Property	**Description/Value**
Sensor/Transducer type	Tipping bucket/reed switch
Precipitation type	Liquid
Accuracy	±2%
Sensitivity	0.2 mm
Closure time	<100 ms (for 0.2 mm of rain)
Capacity	Unlimited
Funnel diameter	225 mm
Standard	400 cm^2
With expander unit	1000 cm^2
Max. current rating	500 mA
Breakdown voltage	400 VDC
Capacity open contacts	0.2 pF
Life (operations)	10^8 closures
Material	Non-corrosive aluminum alloy LM25
Dimensions	390 (h) × 300 (Ø) mm
Weight	2.5 kg
Temperature range (operating)	0…+85 °C

Table 2.4: Specifications of heated rain gauge RG13

Property	**Description/Value**
Sensor/Transducer type	Tipping bucket/reed switch
Accuracy	±2%
Sensitivity	0.2 mm
Closure time	<100 ms (for 0.2 mm of rain)
Capacity	Unlimited
Funnel diameter	225 mm
Standard	400 cm^2
With expander unit	1000 cm^2
Max. current rating	500 mA
Breakdown voltage	400 VDC
Capacity open contacts	0.2 pF
Life (operations)	10^8 closures
Heater	33 W/24 VDC (RG13J)
	33 W/48 VDC (RG13H)
Thermostat operation	Opens at +11 °C (±3 °C)
	Closes at +4 °C (±3 °C)
Material	Non-corrosive aluminum alloy LM25
Dimensions	390 (h) × 300 (Ø) mm
Weight	2.5 kg
Temperature range (operating)	-20…+85 °C

2.3.1 Data Pre-processing and Estimation

For training and validation of the models, the daily data were obtained for seven meteorological stations for ten years, from January 1, 2007, to December 31, 2016 from the Meteorological Stations of Turkish Republic of Northern Cyprus. Prior to the modeling, these daily data were first normalized by (Bisht et al., 2015):

$$P_{norm} = \frac{P_{(t)} - P_{\min(t)}}{P_{\max(t)} - P_{\min(t)}} \leq 1 \qquad (2.1)$$

where P_{norm} is the normalized value of the $P_{(t)}$; $P_{\max(t)}$ and $P_{\min(t)}$ are the max and min values of the observed data, respectively. Due to the training and verification goals, data set was divided into two parts. About 70% of whole data were used for calibration and the rest 30% of data for verifying the trained models.

The “Root Mean Square Error (RMSE)” and “Determination Coefficient (DC)” were used to evaluate the prediction efficiency of the models as (Nourani and Andalib 2015):

$$RMSE = \sqrt{\frac{\sum_{i=1}^{n}\left(P_{obs_i}-P_{com_i}\right)^2}{n}} \tag{2.2}$$

$$DC = 1 - \frac{\sum_{i=1}^{n}(P_{obs_i}-P_{com_i})^2}{\sum_{i=1}^{n}(P_{obs_i}-\bar{P}_{obs})^2} \tag{2.3}$$

where *n* is the data number, P_{obs_i} is the observed data, and P_{com_i} is the predicted (computed) data. DC ranges from -∞ to 1 with a perfect score of 1 and RMSE ranges from 0 to +∞ with the perfect value of 0. Any hydro-environmental method may be adequately evaluated by DC and RMSE criteria (Legates and McCabe, 1999).

CHAPTER 3
MATERIALS AND METHODS

3.1 Proposed Methodology

The thesis is divided into two parts, the temporal and spatial stages of modelling as shown in Figure 3.1 and as discussed in the the following sub-sections.

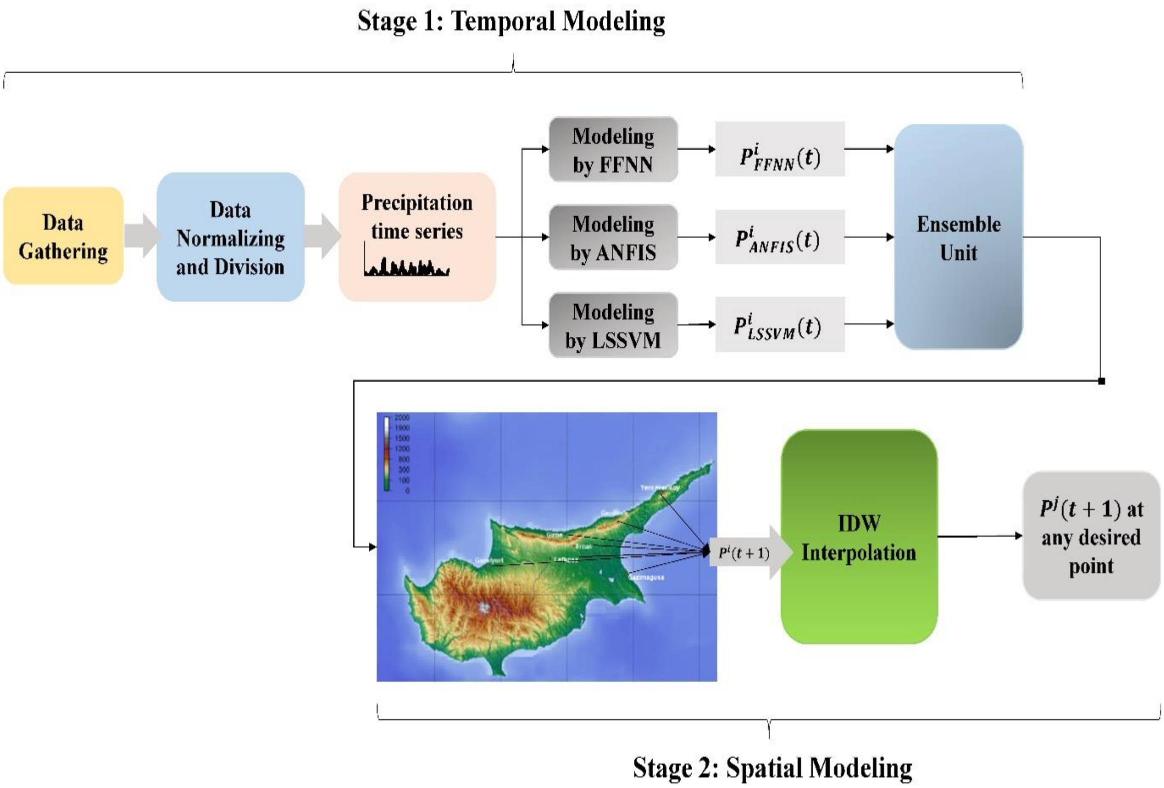

Figure 3.1: Schematic of the proposed methodology (P=precipitation data)

3.2 Artificial Intelligence (AI) Based Temporal Modeling

In the first stage, the monthly precipitation data were normalized by equation (2.1). Three different black box models, ANN (a commonly used AI method), ANFIS (an AI method which serves Fuzzy tools to handle the uncertainties involved in the process) and LSSVM (more recently developed AI model), were separately created on the basis of two different scenarios. Then, outputs of the single models were ensembled using three ensemble techniques as:

(i) simple linear averaging,
(ii) linear weighted averaging,
(iii) non-linear neural ensemble methods.

The inputs of the ensemble unit were outputs of the single models. The modelling was done via two scenarios.

In scenario 1, each station's own data at pervious time steps were used for predicting the same station's precipitation, while in scenario 2, another station's data in addition to each station's data were used for modelling to enhance the prediction performance.

For modeling via the first scenario, the aim was to predict precipitation value using the station values at previous time steps (t-1) and (t-12). So, the prediction of the precipitation could be patterned as:

$$P_t^i = f(P_{t-1}^i, P_{t-12}^i) \tag{3.1}$$

where *i* denotes to the station name (as Ercan, Gazimağusa, Geçitkale , Girne, Guzelyurt, Lefkoşa and Yeni Erenkoy stations) and P_{t-1}^i, P_{t-12}^i are the precipitation values of *i*th station corresponding to time steps *t–1*and *t-12* (or 1 and 12 months ago). The conceptual model of the ensemble system for scenario 1 involving ANN, ANFIS and LSSVM single models is shown by Figure 3.2.

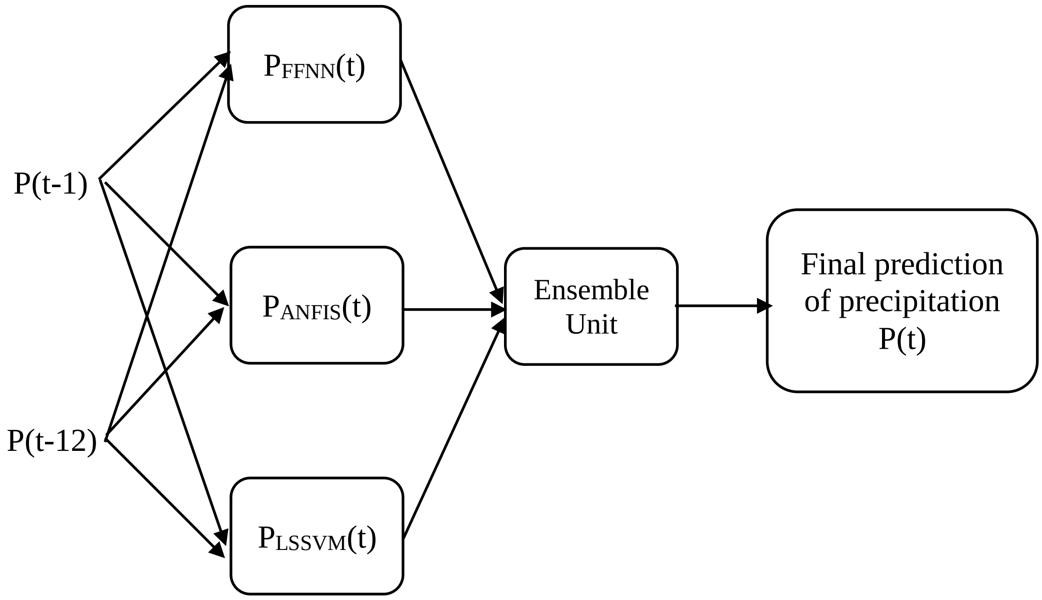

Figure 3.2: Conceptual model of the system in scenario 1

P(t-1) and *P(t-12)* are previous monthly precipitation values corresponding respectively to 1 and 12 months ago; $P_{FFNN}(t)$, $P_{ANFIS}(t)$ and $P_{LSSVM}(t)$ are results of predictions (in current month) by different models. The argumentation of using *P(t-1)* and *P(t-12)* as inputs for prediction of *P(t)* is supported by the following:

a) As shown by some previous studies (Yaseen et al., 2018; Hung et al., 2009; Abbot and Marohasy, 2012) in modeling precipitation, as a Markovian (auto-regression) process, *P(t)* is more correlated with precipitation values at prior time steps as *P(t-1)* and so on. For this reason, it is feasible to select previous time steps values as inputs for the AI models. According to Figure 2.1, and also employing MI, as a non-linear correlating identifier, the lag times of 1 was selected as the dominant input in scenario 1 for all stations.

b) Selection of input *P(t-12)* is related to the seasonality of the precipitation phenomenon. It means that due to the seasonality of the process (i.e. periodicity), the precipitation value of the current month has a strong relation (similarity) with the precipitation level in the same month at previous year. As can be seen in Figure 2.1, the precipitation is much correlated with the precipitation values with the values obtained 12 months ago. It should be noted that the CC could determine the linear correlation between two time series and it is unable to recegnize the non-linear relation. Hence, MI was used to confirm the selection of dominant inputs for the modeling.

In scenario 2, the prediction formula (3.1) was modified by introducing precipitation value from Ercan station P_t^{Ercan} as exogenous input. Therefore, the formula of this scenario expressed as:

$$P_t^i = f(P_{t-1}^i, P_{t-12}^i, P_t^{Ercan}) \tag{3.2}$$

In scenario 2, it was tried to use the data from another station as an exogenous input to enhance the modeling efficiency. In this way, the data from Ercan station were also considered as input data for modeling all other stations.

The argumentation of using precipitation of Ercan Station is explained as:

a) As shown in Table 2.2, Ercan Station has strong non-linear correlation with other station's data.
b) Geographical position of the Ercan Station is central in comparison with the other stations.
c) Ercan Station is installed in strategic and vital importance location main airport of TRNC, requiring more attention in precipitation measurement.

Thus, the data obtained from the Ercan station were considered as exogenous input in the modeling. Employing scenario 2 can be more helpful for forecasting the precipitation of stations when they get out of service (due to technical problems) using their available past observations as well as data from Ercan station.

3.2.1 Feed Forward Neural Network (FFNN)

ANN is based on nonlinear algorithm that finds the relationship for the parameters of a system. ANN is mostly used in water resources and hydrological studies for an estimation tool. In ANN, "Feed Forward (FF) Back Propagation (BP)" network models are common which is a proof that BP model with three-layered, fulfilled for the estimation and simulation (Nourani and Parkizhar, 2013). Three-layered "Feed Forward Neural Network (FFNN)" which were widely used for estimating hydrological time spans, provides a framework for performing the nonlinear functional mapping between a set of input and output, and linear combination of the input variables, which are transformed by a non-linear activation function as expressed by equation (3.3). There is not any loop/cycle in this network. The output value of a FFNN can be obtained through [18]:

$$\hat{y}_k = f_0[\sum_{j=1}^{M_N} W_{kj} \,.\, f_h(\sum_{i=1}^{N_N} W_{ji} X_i + W_{j0}) + W_{k0}] \tag{3.3}$$

where w_{ji} is the applied weight to a neuron in hidden layer which connects *ith* neuron in the inputlayer to the *jth* neuron in the hidden layer, w_{jo} is the applied bias to the *jth* neuron of hidden layer, f_h denotes to the activation function of related hidden layer neuron, w_{kj} indicates the applied weight to a target neuron which connects *jth* hidden neuron to the *kth* target neuron. w_{k0} is the applied bias to the *kth* target neuron, f_0 stands for the activation function of the target neuron, x_i is the *ith* input neuron and y_k and y are respectively the network output and observed values. N_N and M_N respectively show number of input neuron and hidden neurons (Nourani and Komasi, 2013). Hidden and target layers' weights are different from each other and should be estimated during the training phase. The developed ANN structure is shown in Figure 3.3.

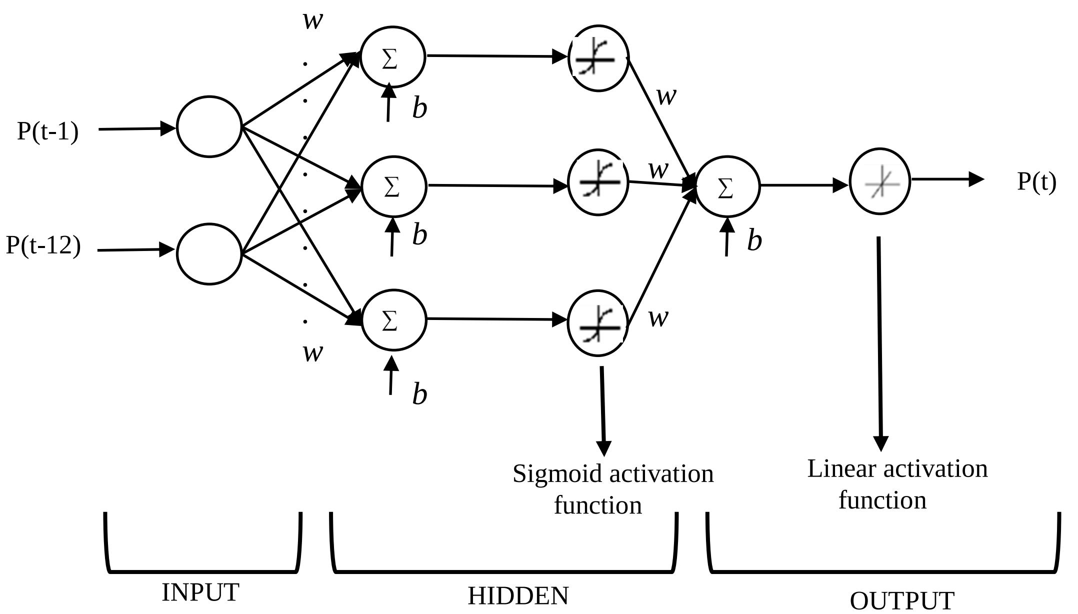

Figure 3.3: Structure of a three-layer feed forward neural network (FFNN)

ANN is widely applied in the hydrological precipitation and water resources. In ANN, BP models are commonly used methodology to engineer. The artificial neural network as an AI-based model is a mathematical model aiming to handle non-linear relationship of input-output dataset. ANN has proved to be effective with regards to complex function in various fields, including prediction, pattern recognition, classification, forecasting, control system and simulation (Govindaraju, 2000). Among the different ANN algorithms, FFNN with BP training is widely applied and is the most common class of ANNs. The term “feed-forward” means that a neuron connection only exists from a neuron in the input layer to other neurons in the hidden layer or from a neuron in the hidden layer to neurons in the output layer and the neurons within a layer are not interconnected to each other. In FFNN-BP, the network is trained by processing the input data through the network and it is transferred to the output layer, and the generated error propagated back to the network until the desired output is archived. The primarily strategy of FFNN-BP is to reduce the error, so that the ANN is trained by the training data set and can predict the correct output (ASCE Task Committee, 2000). So called a BP network model which is the FFNN structure and a BP algorithm. It has proved that BP network model with three-layer is satisfied for the forecasting and simulating in the science of water (ASCE Task Committee, 2000). FFNN includes three layers of input, hidden and output. In this study the input layer consisted of combinations of *P(t-1), P(t-12)* and the target was *P(t)* as shown in Figure 3.2. Both the architecture (the number of neurons, number of layers, transfer function) and learning rate is usually determined using the trial-and error process. The sigmoid activation function was employed for input and hidden layers while in the output layer, a linear function was applied in the used FFNN models. The developed ANN structure illustrated by Figure 3.2.

As shown in Figure 3.2, three-layered feed forward neural networks (FFNNs), which have been usually used in forecasting hydrologic time series, provide a general framework for representing nonlinear functional mapping between a set of input and output variables. Three-layered FFNNs are based on a linear combination of the input variables, which are transformed by a nonlinear activation function.

3.2.2 Adaptive Neuro-Fuzzy Inference System (ANFIS)

ANFIS is a type of ANN, depend on TSK FIS. ANFIS merges the ANN and FL concepts to benefits of both within a unique framework. Fuzzy systems need information to define fuzzy rules and tuning the membership functions parameters. However, ANFISs have more computational restrictions than ANNs (Nourani et. al., 2012). In ANFIS, TSK type FIS is usually used. ANFIS used in this study has two inputs of "P(t-1) and P(t-12)" and one output of P(t) as shown in Figure 3.3. The fuzzy system is combined by three main parts; fuzzification, database, defuzzification whereas the database part includes inference engine and fuzzy rules. Among different fuzzy inference systems which can be used for fuzzy operation, the TSK engine was employed in the current research.

Each fuzzy system contains three main parts, fuzzifier, fuzzy database and defuzzifier. Fuzzy data base contains two main parts, fuzzy rule base, and inference engine. In fuzzy rule base, rules related to fuzzy propositions are described (Jang et al., 1997). Thereafter, analysis operation is applied by fuzzy inference engine. There are several fuzzy inference engines which can be employed for this goal, which Sugeno and Mamdani are the two of well known ones. Neuro-fuzzy simulation refers to the algorithm of applying different learning techniques produced in the neural network literature to fuzzy modeling or a fuzzy inference system (FIS) (Brown and Harris, 1994). This is done by fuzzification of the input through membership functions (MFs), where a curved relationship maps the input value within the interval of [0,1]. The parameters associated with input as well as output membership functions are trained using a technique like backpropagation and/or least squares. Therefore, unlike the multi-layer perceptron (MLP), where weights are tuned, in ANFIS, fuzzy language rules or conditional (if–then) statements, are determined in order to train the model (Rajaee et al., 2009). The ANFIS is a universal approximator and as such is capable of approximat ing any real continuous function on a compact set to any degree of accuracy. The ANFIS is functionally equivalent to fuzzy inference systems (Jang et al., 1997). Specifically, the ANFIS system of interest here is functionally equivalent to the Sugeno first-order fuzzy model (Jang et al., 1997). The general construction of the ANFIS is presented in Figure 3.4.

Figure 3.4 shows the fuzzy reasoning mechanism for the Sugeno model to derive an output function *f* from a given input vector [*P(t-1), P(t-12)*]. The developed ANFIS consists of two inputs of *P(t-1)*, *P(t-12)* and one output of *P(t)* as shown in Figure 3.4. Among different FISs used as fuzzy operations, the Takagi-Sugeno-Kang (TSK) engine was employed in the current research. The corresponding equivalent ANFIS construction is shown in Figure 3.4. According to this figure, it is assumed that the FIS has two inputs *P(t-1)* and *P(t-12)* and one output x(t).

The operation of ANFIS to create target function with 2 input vectors of *P(t-1)*, *P(t-12)* and the first order of TSK applied to 2 fuzzy rules expressed as (Aqil et al., 2007; Sojitra et al., 2015):

Rule (1): if μ(P(t-1)) is A1 and μ(P(t-12)) is B1then f1=p1(P(t-1)) + t1(P(t-12)) + r1

Rule (2): if μ(P(t-1)) is A2 and μ(P(t-12)) is B2 then f1=p2(P(t-1)) + t2(P(t-12)) + r2

A1, *A2*, and *B1*, *B2* are membership functions parameters, for inputs *P(t-1)* and *P(t-12)* and *p1*, *t1*, *r1* and *p2*, *t2*, *r2* are outlet functions' variables, the structure and formulation of ANFIS follows a five-layer neural network structure. For more explanation of ANFIS, refer to the studies of (Jang and Sun, 1997). The conjuction of ANN and fuzzy system presents a robust hybrid system which is capable of solving complex nature of the relationships (Akrami et al., 2014). ANFIS is a Multi-Layer Feed-Forward (MLFF) neural network that is capable of integrating the knowledge of ANN and fuzzy logic algorithm which maps the set of inputs with the outputs. ANFIS as AI-based model employs the hybrid training algorithm which consist of a combination of BP and least squares method (Parmar and Bhardwaj, 2015). The schematic of the ANFIS model is shown by Figure 3.4.

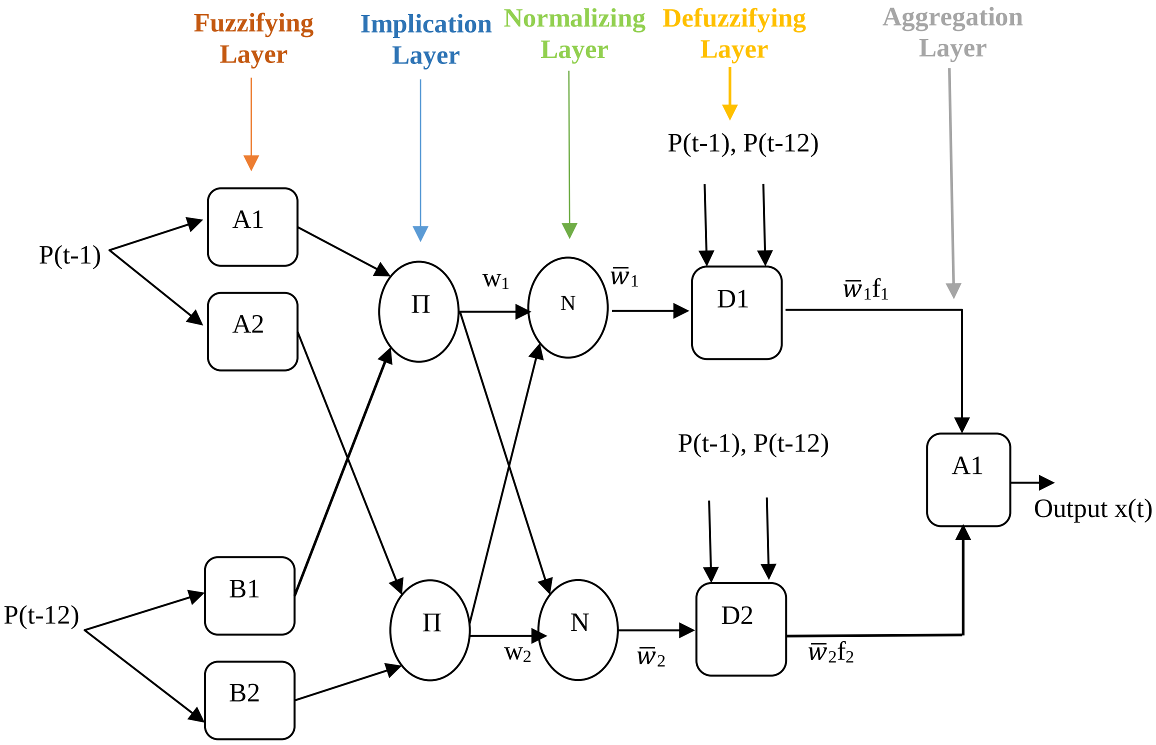

Figure 3.4: ANFIS structure

<u>*Layer 1 (Fuzzyfing Layer):*</u> Each node generates membership values of an input variable. The output of ith node in layer k is denoted as ${Q^k}_i$. For a generalized bellfunction (gbellmf) with MF parameters of {ai, bi, ci}, the output ${Q^1}_i$ can be calculated as:

$$Q_i^1 = \mu_{Ai}(x) = \frac{1}{1+(\frac{x-c_i}{a_i})^{2b_i}} \qquad (3.4)$$

<u>*Layer 2 (Implication Layer):*</u> The imposed signal to the layer is multiplied by each node of this layer as:

$$Q_i^2 = w_i = \mu_{A_i}(x(t-1)).\mu_{B_i}(x(t-12)); i = 1,2,3 \qquad (3.5)$$

Layer 3 (Normalizing Layer): Node i in this layer computes the normalized firing strength:

$$Q_i^3 = \overline{w_1} = \frac{w_i}{w_1+w_2+w_3};\ i = 1,2,3 \tag{3.6}$$

Layer 4 (Defuzzifying Layer): The contribution of ith rule towards the target is determined where, $\bar{w}$ is the output of layer 3 and {pi, qi, ri} is the parameter set:

$$Q_i^4 = \bar{w}_{\mathrm{i}}(p_i x(t-1) + q_i x(t-12) + r_{\mathrm{i}}) = \bar{w}_{\mathrm{i}} f_i \tag{3.7}$$

Layer 5 (Aggregation Layer): Finally, the output of the model is calculated by:

$$Q_i^5 = \overline{w_1}(p_i x(t-1) + q_i x(t-12) + r_i) = \textstyle\sum_i \overline{w_1} f_i \tag{3.8}$$

To estimate the primary parameters set {ai, bi, ci} and consequence parameters set {pi, qi, ri} of the ANFIS, the conjunction of the least squared and gradient descent methods are used as a hybrid calibration algorithm. The ANFIS models proposed in this study were trained using Gaussian and Generalizedbell MF, SugenoFuzzy model.

3.2.3 Least Square Support Vector Machine (LSSVM)

Learning in the context of SVM was proposed and introduced by (Cortes and Vapnik, 1995), which provides a satisfactory approach to the problems of prediction, classification, regression and pattern recognition. SVM is based on the concept of machine learning which consists of data-driven model (Cortes and Vapnik, 1995). The structural risk minimization and statistical learning theory are two useful functions of SVM which make it different from ANN because of its ability to reduce the error, complexity and increases the generalization performance of the network. Generally, SVM is categorized into linear support vector regression (L-SVM) and non-linear support vector regression (N-SVM) (Granata et al., 2017). Therefore, support vector regression (SVM) is a form of SVM based on the two basic structural layers; the first layer is kernel function weighting on the input variable while the second function is the weighted sum of kernel outputs (Cortes and Vapnik, 1995). In SVM, first a linear regression is fitted to the data and thereafter, the outcomes are passed through a non-linear kernel function to map non-linear patterns involved in the data set. The Least Squares formulation of SVM is called LSSVM. Thus, the solution in this method is obtained through solving a linear equations system. Efficient algorithms can be used in LSSVM can be calculated as (Singh et al., 2016):

$$y = f(x) = w^T \varphi(x) + b \tag{3.9}$$

in which f shows relation among the input and output data, w is an m-dimensional weight vector, φ denotes to kernel function mapping input vector x to an m-dimensional feature vector; b stands for the bias. The regression problem can be given as follows (Lu & Wang 2011):

$$\min J(w, b, e) = \frac{1}{2} w^T w + \frac{\gamma}{2} \sum_{i=1}^{m} e_i^2 \tag{3.10}$$

which has the following constraints:

$$y_{i=} w^T \varphi(X_i) + b + e_i \quad (i = 1,2, \dots, m) \tag{3.11}$$

Where γ is the margin parameter and e_i is the slack variable for X_i. To solve the optimization problem, the objective function may be achieved by altering the constraint problem to the unconstraint problem, according to the Lagrange multiplier α_i as:

$$L(w, b, e, \alpha) = J(w, b, e) - \sum_{i=1}^{m} \alpha_i \{w^T \varphi(X_i) + b + e_i - y_i\} \tag{3.12}$$

Vector w in Eq. (8) should be calculated after solution of the optimization problem in the form of (Lu and Wang, 2011):

$$w = \sum_{i=1}^{N} \alpha_i \varphi(x_i) \tag{3.13}$$

Therefore, the ultimate formula for LSSVM could be written in the form of:

$$f(x, \alpha_i) = \sum_{i=1}^{N} \alpha_i P(x, x_i) + b \tag{3.14}$$

where $P(x,x_i)$ shows kernel function which perform nonlinear mapping to the feature space. The Gaussian Radial Basis Function (RBF) is the most commonly used kernel function in LSSVM based modeling in the form of (Singh et al., 2016):

$$P(x - x_{\mathrm{i}}) = exp(-\gamma \left|\left|x - x_{\mathrm{i}}\right|\right|^2) \tag{3.15}$$

where γ and σ are the parameters of the kernel function. Figure 3.5 shows the structure of the LSSVM.

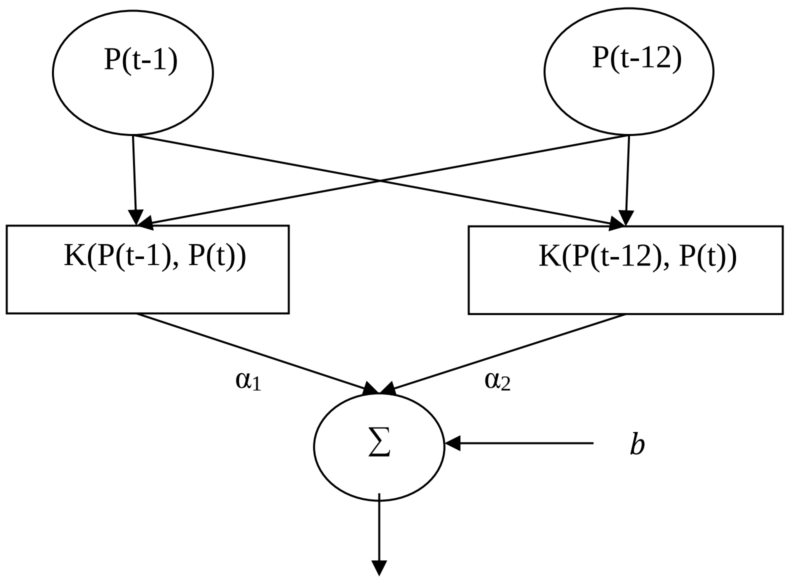

$$y = P(t) = \sum_{i=1}^{3} \alpha_i P(x_i, x) + b$$

Figure 3.5: Structure of LSSVM

3.3 Ensemble Unit

Clearly the combining the outputs from several prediction methods can improve the final accuracy of a time series modeling tool. In an ensembling process the outcomes of various models are used and as so, the final outputs will not be sensitive to selection of the best methods. Therefore, predicts of ensemble method will be more safe and less risky than the results of the single best methods. Various studies at different fields of engineering suggested to ensemble outcomes of several methods as an effective approach to improve the performance of time series predictions (Kasiviswanathan et al., 2013; Zhang and Berardi, 2001).

An ensemble technique as a learning algorithm, gathers a set of classifiers to classify new variables by applying weights on the single prediction values. The goal of such ensemble learning technique is to develop an ensemble of the individual methods that are diverse and yet accurate. In this thesis, three ensemble techniques were applied to combine of the outputs of the used AI based models to enhance the overall efficiency of the predictions as:

3.3.1 Simple averaging

a) the simple linear averaging method:

$$\bar{P}(t) = \frac{1}{N}\sum_{i=1}^{N} P_i(t) \qquad (3.16)$$

where $\bar{P}(t)$ is the output of the simple ensemble model, N shows the number of single models (in this study, N=3) and $P_i(t)$ stands for the outcome of the ith method (i.e. ANN, ANFIS and LSSVM) in time step t.

3.3.2 Weighted averaging

b) the linear weighted averaging method:

$$\bar{P}(t) = \sum_{i=1}^{N} w_i P_i(t) \qquad (3.17)$$

Where i shows imposed weight on the output of ith method that may be computed on the basis of the performance measure of ith method as:

$$w_i = \frac{DC_i}{\sum_{i=1}^{N} DC_i} \qquad (3.18)$$

Where DC_i measures the model efficiency (such as coefficient of determination).

3.3.3 Non-linear averaging

c) the non-linear neural ensemble method:

For the nonlinear ensemble method another FFNN model is trained by feeding the outputs of single AI models as inputs to the neurons of the input layer (see Figure 3.6). Number of hidden layer neurons and maximum epoch numbers are defined through trial-error procedure.

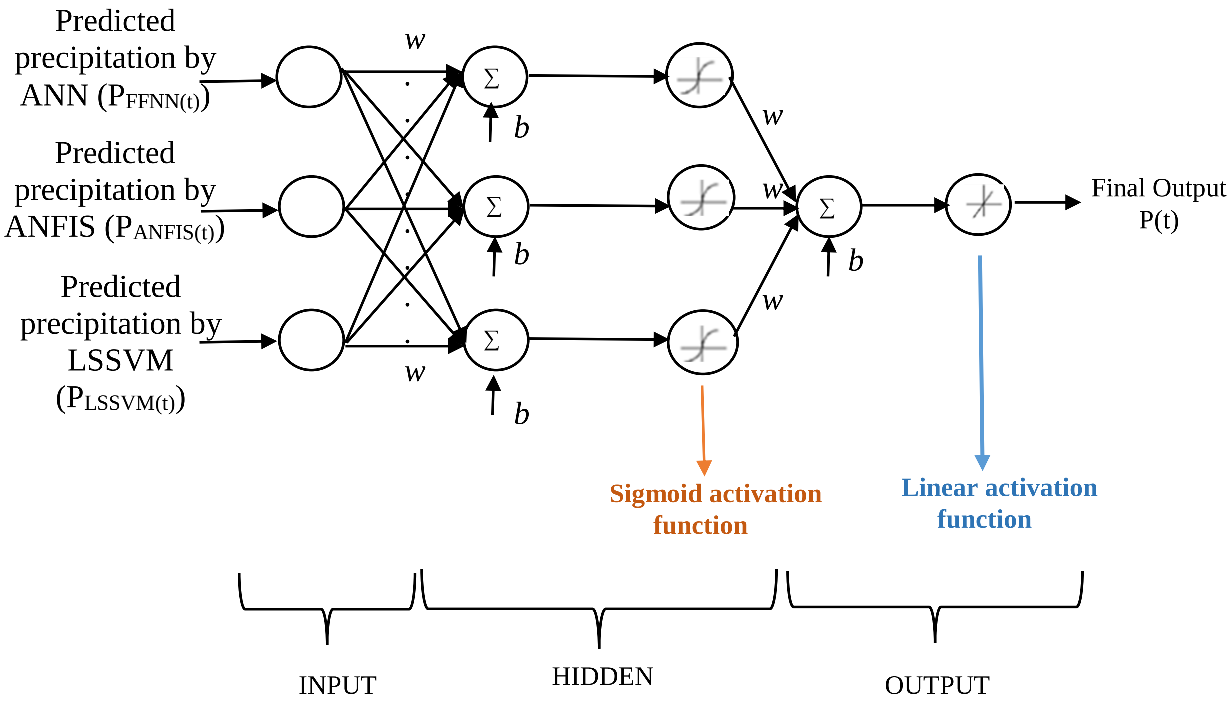

Figure 3.6 Schematic of the proposed neural ensemble method

3.4 Spatial Modeling

In recent years, Geographical Information Systems (GIS) for spatial interpolation and prediction of precipitation has acquired increasing popularity. For many interpolation, approximation and prediction methods were developed to predict values of spatial phenomena in unsampled locations and also different methods can produce different spatial representations. (for reviews see Burrough 1986; Franke and Nielson 1991) For example, in local neighbourhood approach, local methods are based on the assumption that each point influences the resulting surface only up to a certain finite distance. Values at different unsampled points are computed by functions with different parameters, and the condition of continuity between these functions is defined only for some approaches. The method of point selection used for the computation of the interpolating function differs among the various methods and their concrete implementations.

3.4.1 Inverse distance weighted (IDW) interpolation

This is one of the most useful, simplest and most readily available methods. It is based on an assumption that the value at an unmeasured point can be approximated as a weighted average of values at points within a certain cut-off distance, or from a given number m of the closest points. IDW interpolation is mathematical assuming closer values are more related than further values with its function. Weights are usually inversely proportional to a power of distance.

Spatial autocorrelation is the underlying assumption of Inverse Distance Weighting. For example, some points have known elevation values. The other points will be interpolated. If you wanted to measure the A point, you can set up your interpolation so that it takes a fixed or variable number of points. Interpolated points are estimated based on their distance from known cell values. Points that are closer to known values will be more influenced than points that are farther away.

In the thesis, as a second stage for spatial modeling, the predicted values of precipitation at different stations in the first stage were imposed into the IDW method in order to estimate precipitation at any desired point within the study area. In order to evaluate the spatial interpolation as well as overall efficiency of the proposed hybrid spatiotemporal modelling framework, cross-validation technique was considered in this study. Cross-validation is a process for checking the adaptability between a set of data, the spatial model and neighborhood design (Isaaks and Srivastava, 1989). In cross-validation, each station in the spatial model is individually removed from the model, and then it’s value is estimated by the spatial interpolator. In this way, one station set aside and the created time series models (ensemble technique) of other stations are used to predict the precipitation values of the stations time step by time step for the verification period. Then the predicted values of these stations are used in the IDW method to estimate the precipitation values of that station (set aside) for the validation period. The obtained verification time series can then be compared with the observed verification time series of that station. This procedure is repeated for all other stations similarly to evaluate the overall efficiency of the method. In this way, a spatial interpolation tool must be created employing predicted values of precipitation from six other stations for estimating precipitation at the desired station (set aside). In this study, IDW method was used for the spatial interpolation purpose.

The IDW as a deterministic multivariate interpolation method is based on the assumption that the attribute value of an un-sampled point is the weighted average of known values within the neighborhood (Lu & Wong 2008). In the IDW method, the weightings are solely a function of the distance between the point of interest and the sampling points for (*i=1, 2, …, n)*. Considering the distance D_i between these two points, the value of a point of interest point takes the form:

$$Z = \frac{\sum_{i=1}^{n} \frac{1}{D_i{}^q} Z_i}{\frac{1}{D_i{}^q}} \tag{3.19}$$

where Z is the interpolated value of the point of interest; Z_i is the value of sampling point i; D_i is the distance between the interpolated and sampled values; and q is an appropriate constant. If the parameter q takes a value of 1 or 2, the method is called, respectively, inverse distance interpolation or inverse distance squared interpolation (Ashraf et al. 1997).

CHAPTER 4
RESULTS AND DISCUSSION

4.1 Results of Temporal Modeling

For the temporal modeling firstly single AI based methods were trained and verified via two different input scenarios and then the prediction efficiency of AI based modeling was enhanced using ensemble techniques. The obtained results for both single and ensemble modeling are presented in the following sub-sections.

At the first step, FFNN, ANFIS and LSSVM models were separately created via the proposed scenarios 1 and 2. For precipitation prediction of the stations, monthly precipitation values were individually imposed into ANN, ANFIS and LSSVM models in order to predict one-month-ahead precipitation. For this purpose, the ANN, ANFIS and LSSVM models' architectures set dependent on the priority of the precipitation process.

The monthly precipitation data are described by both Markovian and seasonal properties (Kisi and Cimen, 2012). For this reason, the current precipitation *P(t)* is related to its previous time steps, *P(t-1),* as well as its value at twelve months ago, *P(t-12)*. Consequently, the input values as *P(t-1)* and *P(t-12)* were applied to the FFNN, ANFIS and LSSVM models to predict precipitation at time step *P(t)*, for scenario 1 (including more lagged precipitation values, i.e., *P(t-2)* and *P(t-3)* did not show higher MI with output and could not improve the efficiency of the modeling). For scenario 2, one more input, Ercan’s station precipitation value as exogenous input, was also considered (in addition to the input of scenario 1) as another input neuron to enhance the prediction performance.

4.1.1 Results of single AI models

4.1.1.1 Results of FFNN model

To prevent the FFNNs from overtraining issue, it is important to select optimum number of hidden neurons as well as training iteration (epoch) number. Levenberg Marquardt scheme (Hagan and Menhaj, 1996) as training algorithm and 10–300 training epoch numbers and 1–30 hidden neurons were examined to develop the FFNN models. The best results by FFNN models for precipitation modeling of all stations are shown in Table 4.1 for both scenarios 1 and 2.

Table 4.1: Results of monthly precipitation predictions by FFNN for both scenarios 1 and 2

Station	Scenario	Epoch	Network Structure [a]	DC		RMSE (normalized)	
				Calibration	Verification	Calibration	Verification
Ercan	1	20	(3.14.1)	0.670	0.637	0.176	0.157
Gazimağusa	1	60	(3.2.1)	0.547	0.538	0.183	0.120
	2	10	(4.10.1)	0.766	0.684	0.144	0.106
Geçitkale	1	90	(3.4.1)	0.673	0.503	0.147	0.099
	2	20	(4.11.1)	0.845	0.677	0.108	0.087
Girne	1	30	(3.16.1)	0.729	0.511	0.119	0.169
	2	10	(4.12.1)	0.800	0.728	0.101	0.135
Güzelyurt	1	10	(3.5.1)	0.723	0.423	0.150	0.145
	2	10	(4.18.1)	0.854	0.664	0.114	0.131
Lefkoşa	1	20	(3.17.1)	0.585	0.545	0.172	0.138
	2	10	(4.3.1)	0.768	0.621	0.142	0.124
Yeni Erenköy	1	40	(3.4.1)	0.570	0.474	0.134	0.079
	2	20	(4.11.1)	0.835	0.692	0.090	0.069

[a]Only the resuts of the optimime models have been tabluated. In network structure (a.b.c) ab,c respectively show the numbers of input,hidden and output nerouns.

4.1.1.2 Results of ANFIS models

To train the ANFIS models, the Sugeno FIS engine was used in the modeling framework. Each ANFIS should include some rules and membership functions. In this thesis, Gaussian-shaped and 2 Gaussian combinations MFs, as well as the Triangular-shaped and pi-shaped MFs were found to be appropriate for monthly precipitation modeling. Furthermore, the constant MF was applied in the output layer of the ANFIS models. Not only the number of membership functions but also the number of training epochs were examined to reach to the optimum ANFIS models. The ranges of 5–300 and 2–5 were considered respectively for the numbers of training epoch and membership functions. The best results for the ANFIS models are shown in Table 4.2 for all stations via both scenarios 1 and 2.

Table 4.2: Results of monthly precipitation predictions by ANFIS model both scenarios 1 and 2

Station	Scenario	Epoch	Network Structure [a]	DC		RMSE (normalized)	
				Calibration	Verification	Calibration	Verification
Ercan	1	5	trimf-2	0.591	0.582	0.195	0.162
Gazimağusa	1	35	trimf-2	0.510	0.479	0.188	0.126
	2	80	pimf-2	0.823	0.633	0.104	0.117
Geçitkale	1	10	trimf-3	0.728	0.483	0.127	0.102
	2	5	gauss2mf-2	0.840	0.630	0.107	0.099
Girne	1	75	trimf-2	0.716	0.439	0.111	0.180
	2	5	trimf-2	0.876	0.678	0.075	0.158
Güzelyurt	1	95	trimf-2	0.700	0.418	0.128	0.148
	2	5	trimf-2	0.893	0.645	0.071	0.144
Lefkoşa	1	100	trimf-2	0.554	0.515	0.176	0.137
	2	5	trimf-2	0.869	0.609	0.092	0.135
Yeni Erenköy	1	15	gaussmf-2	0.617	0.447	0.127	0.082
	2	10	gaussmf-2	0.899	0.617	0.071	0.074

[a] trimf: Triangular-shaped MF gaussmf: Gaussian MF; gauss2mf: two Gaussian combination MF; pimf: pi shaped MF

4.1.1.3 Results of LSSVM models

Thereafter, the LSSVM models were created to predict the precipitation time series of the stations using RBF kernel. Several studies have already reported more reliable results of LSSVM model using RBF kernel with regard to using other kernels maybe due to its smoothness assumption (Singh et al., 2016). The best results obtained by LSSVM in modeling the precipitation of the stations are shown in Table 4.3 for both scenarios 1 and 2.

Table 4.3: Results of monthly prediction of precipitation by LSSVM model for both scenarios 1 and 2

Station	Scenario	Network Structure [a]	DC		RMSE (normalized)	
			Calibration	Verification	Calibration	Verification
Ercan	1	(10,2,0.1)	0.655	0.556	0.184	0.162
Gazimağusa	1	(10,0.3,0.3333)	0.550	0.497	0.185	0.123
	2	(10,0.3,0.3333)	0.816	0.680	0.129	0.115
Geçitkale	1	(20,0.1,1)	0.676	0.507	0.150	0.102
	2	(20,0.1,1)	0.866	0.654	0.089	0.110
Girne	1	(50,0.01,0.3333)	0.704	0.502	0.123	0.177
	2	(50,0.01,0.3333)	0.876	0.701	0.085	0.148
Güzelyurt	1	(1,0.2,0.3333)	0.727	0.415	0.156	0.143
	2	(1,0.2,0.3333)	0.894	0.657	0.109	0.122
Lefkoşa	1	(60,0.2,0.5)	0.582	0.530	0.173	0.142
	2	(60,0.2,0.5)	0.769	0.588	0.098	0.139
Yeni Erenköy	1	(60,0.01,0.3333)	0.619	0.473	0.132	0.084
	2	(60,0.01,0.3333)	0.852	0.670	0.086	0.068

[a] Structure shows (γ, ε, c).

As it is shown by Tables 4.1, 4.2 and 4.3 the results of the methods in scenario 1 show a bit better performance for Ercan and Lefkoşa stations than other stations in the verification phase since these stations are located in central and higher parts of the island in contrast to the other stations which are located in shore lines and are impacted more significantly by the irregular variations of the sea atmosphere. This can also be confirmed by the standard variation values presented in Table 2.1 which shows the lower values for these two stations.

In scenario 2, the models of the Girne station in verification step showed better efficiency than others. This can be due to its proximity to Ercan station. In other words, not only the small distance between Girne and Ercan stations but also the predominant wind directions over the island (which is from northwest to southeast) make the precipitation pattern of both stations more similar with regard to the others. This can also be clearly seen from Table 2.2 which shows higher MI value between these stations.

Considering the outcomes of both scenarios, because of using Ercan station's data as exogenous input (in addition to each station's own data), the results of scenario 2 were better than scenario 1, showing improvement of modeling efficiency up to 61% and 58% in calibration and verification steps, respectively.

For instance, Figures 4.1, 4.2 and 4.3 illustrate the results of single AI methods for the calibration and verification steps and scatter plots for verification step for Ercan and Girne stations based on scenarios 1 and 2, respectively.

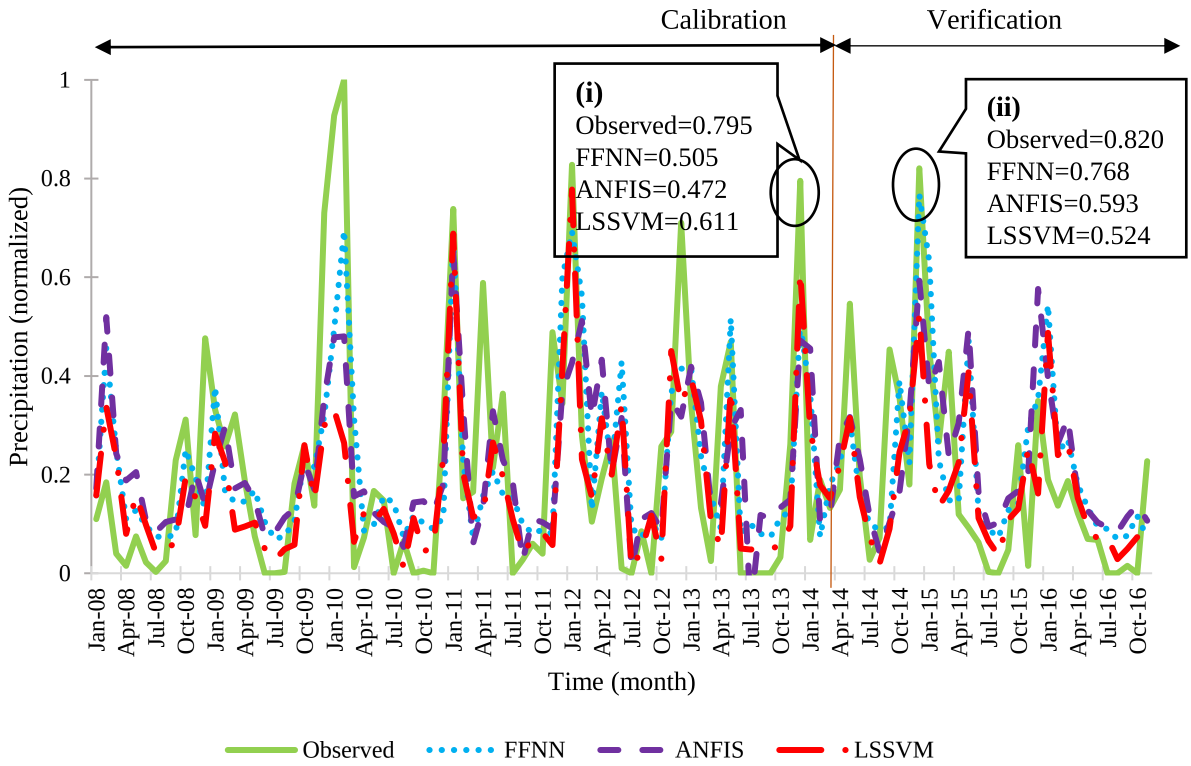

(a) Observed versus computed precipitation time series by FFNN, ANFIS and LSSVM models

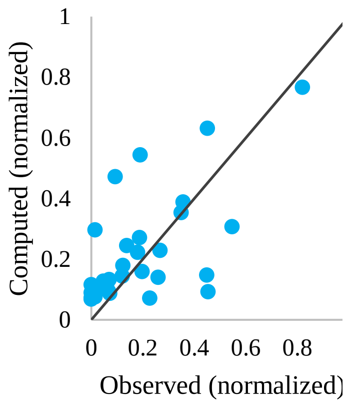

(b) Scatter plots for verification step for FFNN

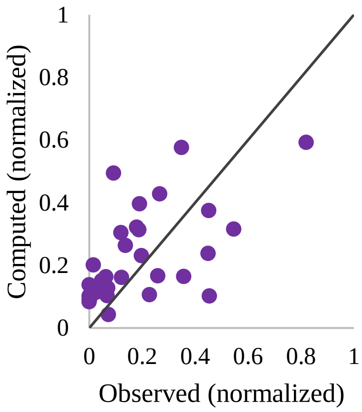

(c) Scatter plots for verification step for ANFIS

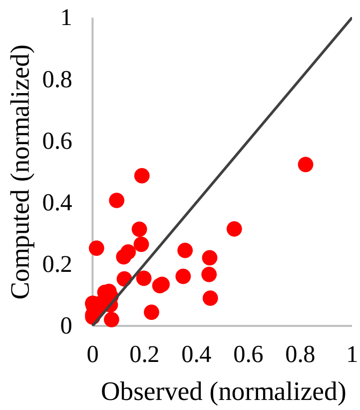

(d) Scatter plots for verification step for LSSVM

Figure 4.1: Time series and scattered plot for FFNN, ANFIS and LSSVM models via scenario1 for Ercan station

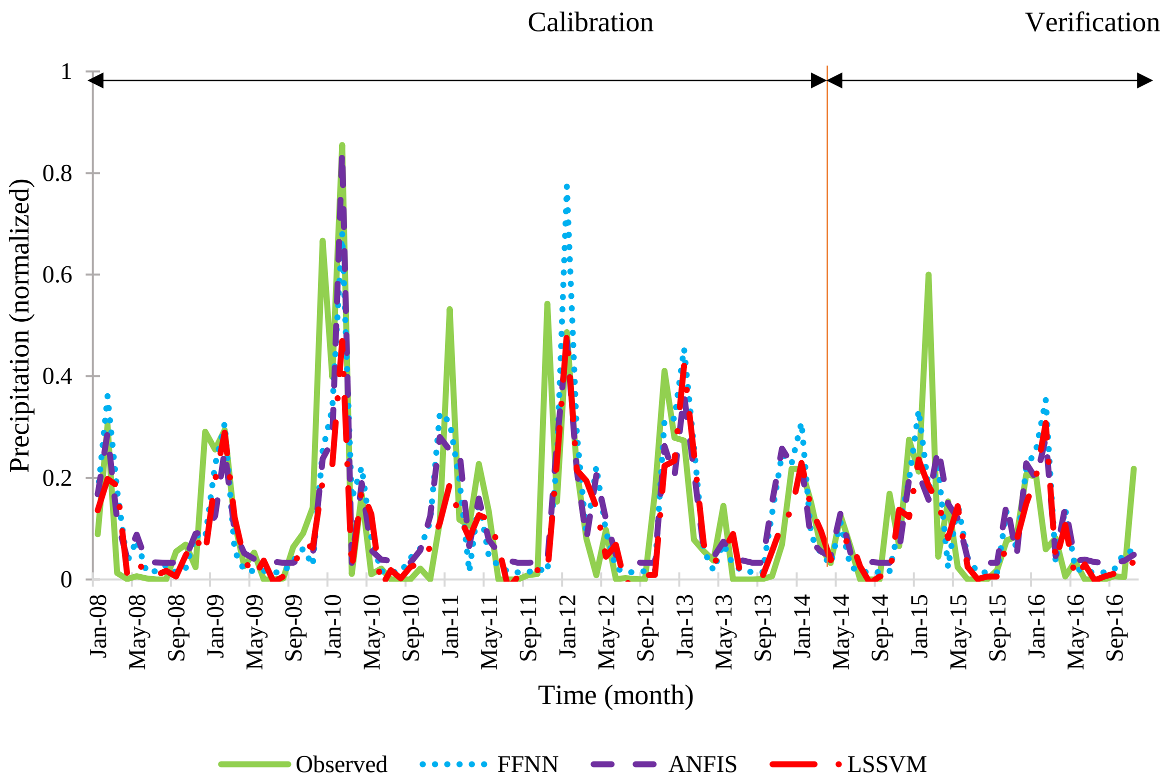

(a) Observed versus computed precipitation time series by FFNN, ANFIS and LSSVM models

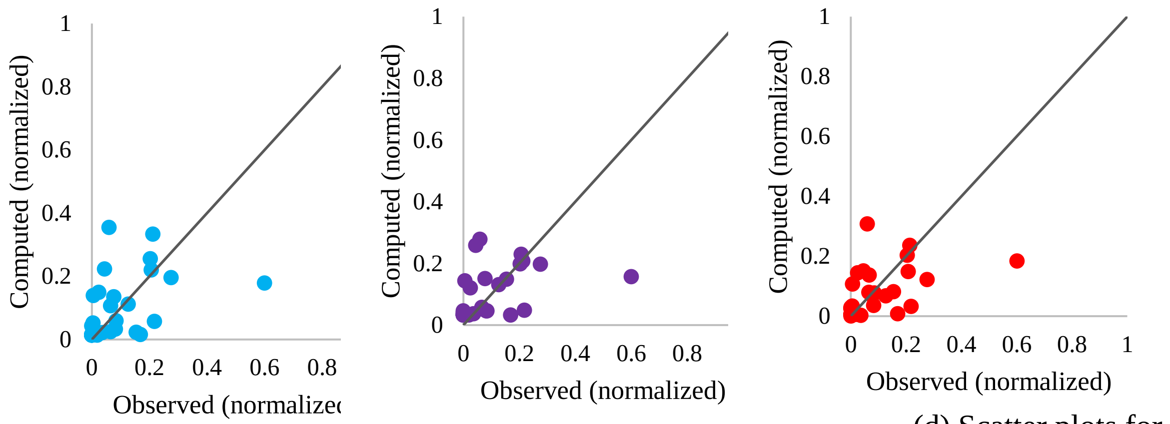

(b) Scatter plots for verification step for FFNN

(c) Scatter plots for verification step for ANFIS

(d) Scatter plots for verification step for LSSVM

Figure 4.2: Time series and scatter plots for verification step for FFNN, ANFIS and LSSVM models via scenario 1 for Girne station

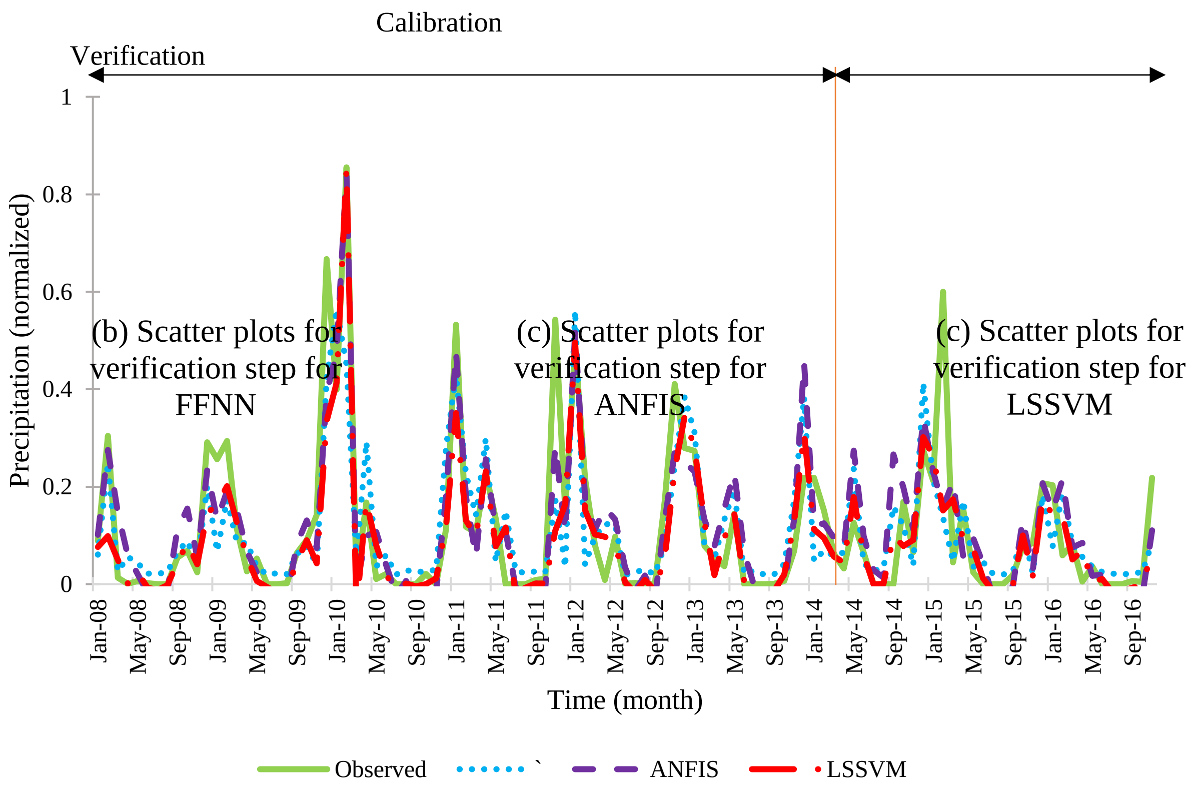

(a) Observed versus computed precipitation time series by FFNN, ANFIS and LSSVM models

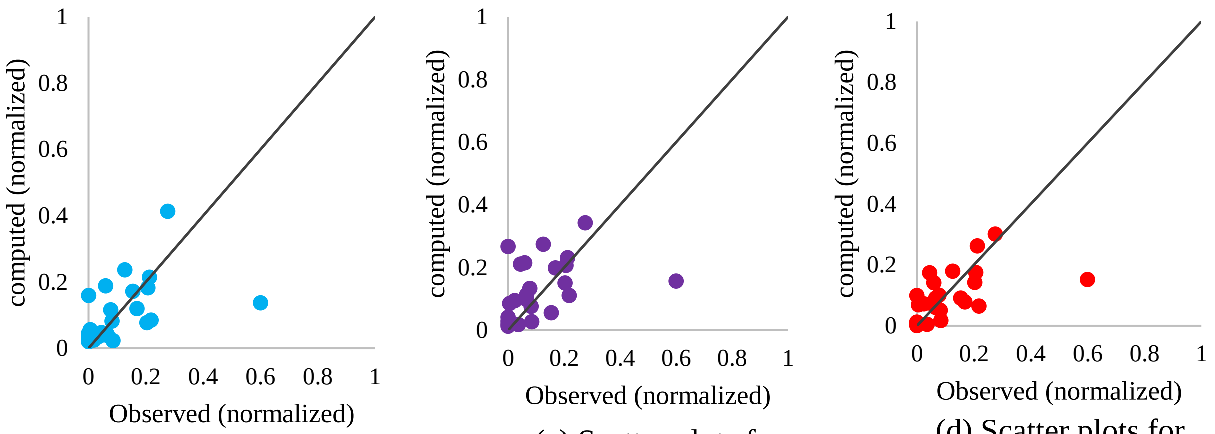

(b) Scatter plots for verification step for FFNN

(c) Scatter plots for verification step for ANFIS

(d) Scatter plots for verification step for LSSVM

Figure 4.3: Time series and scatter plots for verification step for FFNN, ANFIS and LSSVM models via scenario 2 for Girne station

As it can be seen from Tables 4.1, 4.2, 4.3 and Figures 4.1, 4.2, 4.3, generally in most cases, the performance of FFNN was better than other models, however in some cases, the ANFIS and in some other cases LSSVM's performance was better than others. Also, comparison of the outputs obtained by the single AI methods (Figures 4.1, 4.2, 4.3) shows that in different parts of the time series, some of the models led to over estimations and others down estimations of the observed time series. Figure 4.1 (a) highlights 2 points (i) and (ii). According to the figure, it is obvious that for the point (i), LSSVM method provided better fitting to the observed value. However, for sample point (ii), the FFNN model led to the minimum error. In addition, in the interval of November-2009 to March-2010 and November-2012 to January-2013, all models were unable to provide good predictions. Therefore, such different performances of different methods at different sample points and time spans confirms a need to ensemble the results of the different methods via the ensemble techniques.

4.1.2 Results of ensemble modeling

In the ensemble modeling, the outputs of three AI based single models were combined to improve the prediction performance. In this step, only the verification dataset was employed to compute the weights of the averaging methods. For the neural averaging method, like the single FFNN model, the Levenberg Marquardt algorithm as training algorithm. The ranges of 10–300 and 1–30 respectively for the numbers of training epochs and hidden neurons were examined to obtain the best results. Results of different ensemble methods are shown by Table 4.4 and Table 4.5 respectively for scenarios 1 and 2.

Table 4.4: Results of ensembles using linear, weighted and non-linear averaging methods for scenario 1

Station	Ensemble Method[a]	Model structure[a]	DC		RMSE (normalized)	
			Calibration	Verification	Calibration	Verification
Ercan	Simple linear averaging	-	0.678	0.643	0.177	0.149
	Weighted averaging	0.357-0.331-0.312	0.680	0.644	0.177	0.149
	Non-linear averaging	(3,16,1)	0.786	0.677	0.148	0.146
Gazimağusa	Simple linear averaging	-	0.560	0.520	0.182	0.121
	Weighted averaging	0.347-0.320-0.333	0.559	0.521	0.182	0.121
	Non-linear averaging	(3,3,1)	0.702	0.540	0.155	0.126
Geçitkale	Simple linear averaging	-	0.7431	0.650	0.134	0.094
	Weighted averaging	0.337-0.323-0.340	0.741	0.651	0.135	0.094
	Non-linear averaging	(3,12,1)	0.765	0.670	0.128	0.092
Girne	Simple linear averaging	-	0.753	0.516	0.111	0.173
	Weighted averaging	0.352-0.302-0.346	0.750	0.522	0.112	0.173
	Non-linear averaging	(3,11,1)	0.825	0.678	0.095	0.157
Güzelyurt	Simple linear averaging	-	0.779	0.432	0.139	0.143
	Weighted averaging	0.337-0.333-0.330	0.776	0.433	0.140	0.143
	Non-linear averaging	(3,4,1)	0.774	0.447	0.137	0.143
Lefkoşa	Simple linear averaging	-	0.594	0.561	0.171	0.138
	Weighted averaging	0.343-0.324-0.333	0.592	0.564	0.171	0.138
	Non-linear averaging	(3,2,1)	0.706	0.585	0.150	0.138
Yenierenköy	Simple linear averaging	-	0.628	0.489	0.128	0.081
	Weighted averaging	0.340-0.321-0.339	0.623	0.489	0.129	0.080
	Non-linear averaging	(3,13,1)	0.690	0.491	0.118	0.079

[a]Model structure in weighted averaging method shows applied weights respectively on FFNN, ANFIS and LSSVM outputs, whereas for neural averaging it shows numbers of input, hidden and output neurons, respectively.

Table 4.5. Results of ensembles using linear, weighted and non-linear averaging methods for scenario 2

Station	Ensemble Method	Model structure [a]	DC		RMSE (normalized)	
			Calibration	Verification	Calibration	Verification
Gazimağusa	Simple linear averaging	-	0.851	0.699	0.116	0.107
	Weighted averaging	0.336-0.320-0.344	0.847	0.699	0.118	0.107
	Non-linear averaging	(3,20,1)	0.900	0.722	0.095	0.102
Geçitkale	Simple linear averaging	-	0.880	0.681	0.096	0.096
	Weighted averaging	0.345-0.321-0.334	0.873	0.691	0.099	0.093
	Non-linear averaging	(3,5,1)	0.883	0.727	0.100	0.086
Girne	Simple linear averaging	-	0.889	0.734	0.079	0.144
	Weighted averaging	0.345-0.322-0.333	0.884	0.744	0.080	0.142
	Non-linear averaging	(3,16,1)	0.947	0.813	0.090	0.122
Güzelyurt	Simple linear averaging	-	0.923	0.686	0.089	0.124
	Weighted averaging	0.338-0.328-0.334	0.913	0.681	0.096	0.123
	Non-linear averaging	(3,18,1)	0.885	0.668	0.106	0.121
Lefkoşa	Simple linear averaging	-	0.895	0.627	0.101	0.127
	Weighted averaging	0.342-0.335-0.323	0.884	0.633	0.107	0.125
	Non-linear averaging	(3,17,1)	0.953	0.691	0.064	0.123
Yenierenköy	Simple linear averaging	-	0.884	0.690	0.077	0.067
	Weighted averaging	0.350-0.312-0.338	0.880	0.690	0.078	0.067
	Non-linear averaging	(3,19,1)	0.929	0.787	0.060	0.059

The outputs obtained by the ensemble techniques indicate that almost all three ensemble techniques could produce reliable results in comparison to the single AI methods. For example, Figure 4.4 shows the results of precipitation predictions using the ensemble models for both calibration and verification phases and the scatter plot for the verification step by using the neural ensemble method for Girne station based on the scenario 2.

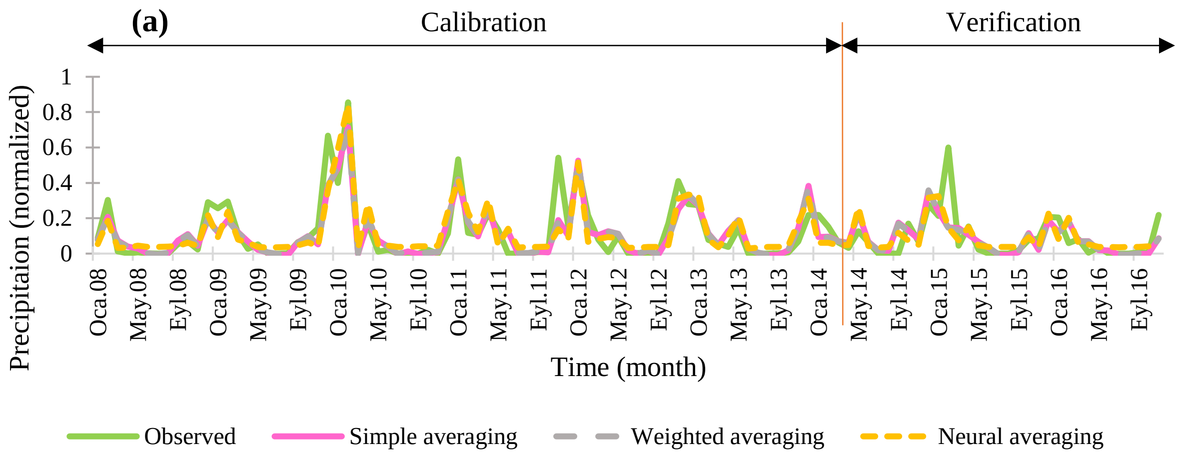

(a) Results of precipitation prediction using simple, weighted and neural averaging methods and observed precipitation.

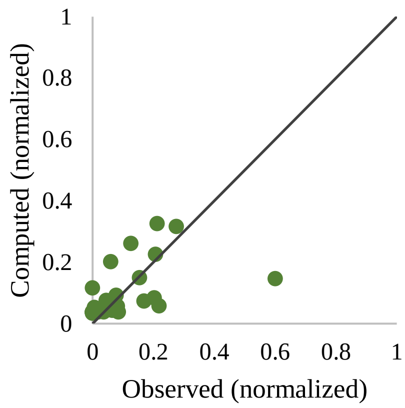

(b) Scatter plots for verification step using neural ensemble method

Figure 4.4: Time series precipitation using simple, weighted and neural averaging methods and observed precipitation using neural ensemble method based on scenario 2 for Girne station.

As mentioned above, any method has its own benefits and drawbacks. Some models may provide over and some others may provide lower estimates. Thus, the ensemble model could lead to better outcomes than the single models because of using the unique capability of each model. It should be noticed that since the outputs of the single methods are close together (see Tables 4.1, 4.2, 4.3), and because the efficiency of simple and weighted averaging ensemble techniques are in the same directs with the single methods, outputs of simple and weighted ensemble techniques are almost quite same. As it can be seen from Tables 4.4, 4.5

and Figure 4.4, the efficiency of neural ensemble is better than the linear ensembling methods in most cases.

For instance, the scatter plot of FFNN and neural ensemble method based on scenario 2 for Girne station at verification step is presented in Figure 4.5.

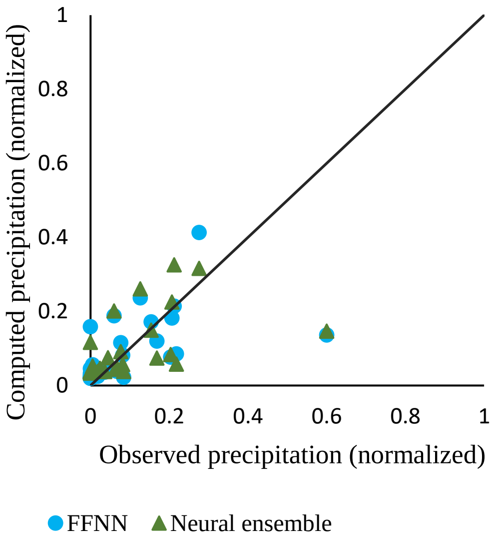

Figure 4.5: Scatter plot for verification step using FFNN and neural ensemble method based on scenario 2 for Girne station

In terms of DC, simple linear, weighted linear and non-linear neural averaging methods enhanced the predicting performance up to 15%, 15%, 38% and 16%, 15%, 24% in calibration step for scenarios 1 and 2 and up to 35%, 35%, 54% and 12%, 12%, 28% in verification step for scenarios 1 and 2, respectively. It's obvious that the neural ensemble could lead to better results by 10% on average. Furthermore, the ensembling model could improve the efficiency of precipitation modelling of Girne station more than other stations by 21% on average in the verification step. On the other hand, this method could not improve the modelling efficiency of Güzelyurt station meaningfully.

4.2 Results of Spatial Modeling

For cross-validation purpose, the IDW based interpolator was conducted for all seven stations. To estimate the precipitation values of each station, the best temporal predictions (obtained by neural ensemble technique via scenario1) for other stations were imposed to the IDW method time step by time step for the verification period. Table 4.6 summarises the cross-validation results for all stations and the overall (mean) efficiency of the proposed ensemble time-space modelling.

Table 4.6: Cross-validation results for the proposed spatiotemporal modeling

Station	DC	RMSE (normalized)
Ercan	0.601	0.234
Gazimağusa	0.758	0.115
Geçitkale	0.629	0.146
Girne	0.558	0.194
Güzelyurt	0.766	0.111
Lefkoşa	0.800	0.133
Yeni erenköy	0.584	0.131
Mean	**0.700**	**0.152**

Results of Table 4.6 show an acceptable performance of Geostatistical IDW tool in spatial simulation of monthly precipitation. Furthermore, among seven different stations, IDW method could estimate the precipitation of Lefkoşa station more accurate than others. The superior results of Lefkoşa station can be due to its higher MI values with other stations (Table 2.2) which show higher nonlinear correlation of its precipitation values with other stations. Unlike temporal modelling, in spatial IDW method for simulating spatial pattern of precipitation, each station's own data are not employed for the modelling but the predicted values of other stations are used. Therefore, it might be supposed that the neural averaging results to be better than spatial stage results. By comparing the results of spatial stage with results of neural averaging method of temporal stage (Tables 4.4 and 4.6), surprisingly it was found that for Gazimağusa, Güzelyurt, Lefkoşa and Yeni Erenköy stations, the results of spatial stage are a bit more accurate than the results of neural averaging method (scenario 1 of temporal stage). Also, the results for Gazimağusa, Güzelyurt and Lefkoşa stations are better than the results of neural averaging method obtained via scenario 2 of temporal modelling stage which in this scenario not only temporal data (each station's own data) but also Ercan station's data as spatial exogenious input were employed in the modeling. This can be due to this fact that the time series of these stations may contain more noises and since in IDW method, data of other stations (not each station's own data) were employed for modeling, so the efficiency of spatial modelling was a bit higher than temporal modelling.

For example, spatial maps for October-2014, August-2016 and also annual average of year 2015 are drawn for precipitation values to identify the variation in the results predicted by space–time model (see Figure 4.6). Such maps can be useful for designing hydraulic structures and also water resources management.

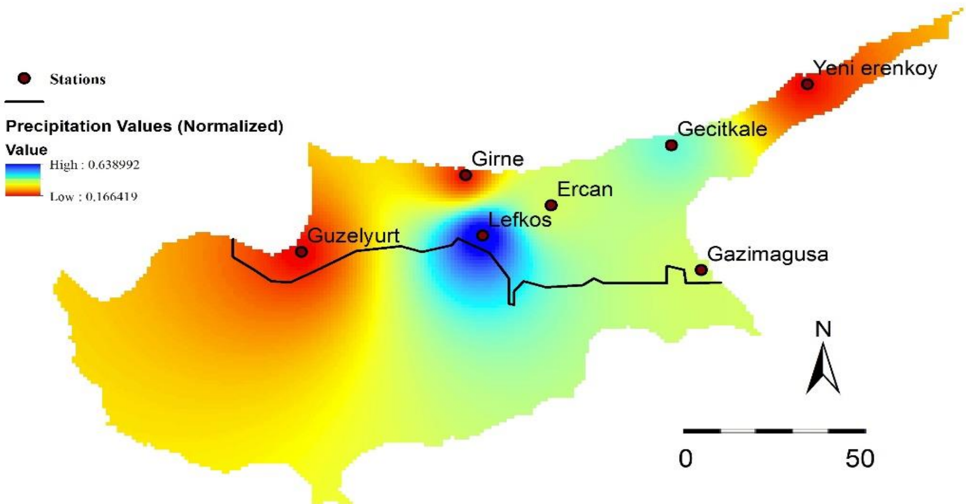

(a) Spatial precipitation distribution for October-2014

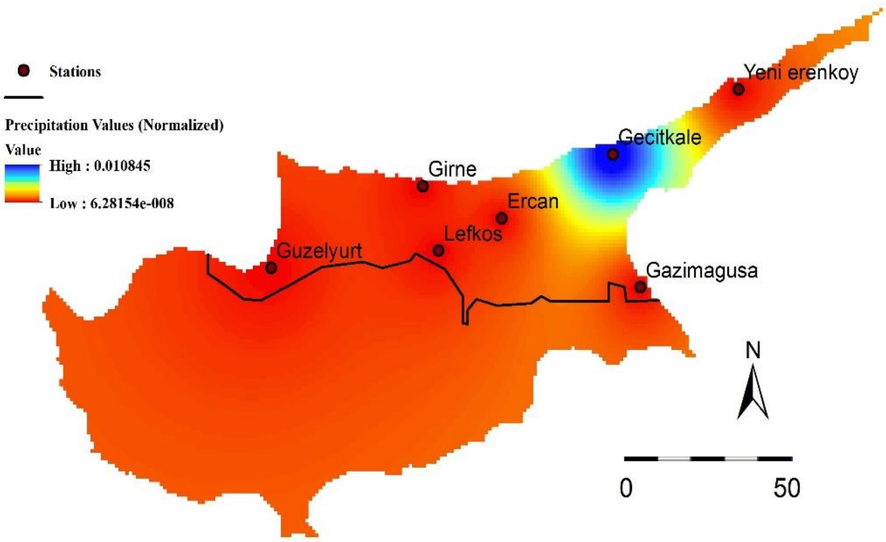

(b) Spatial precipitation distribution for August-2016

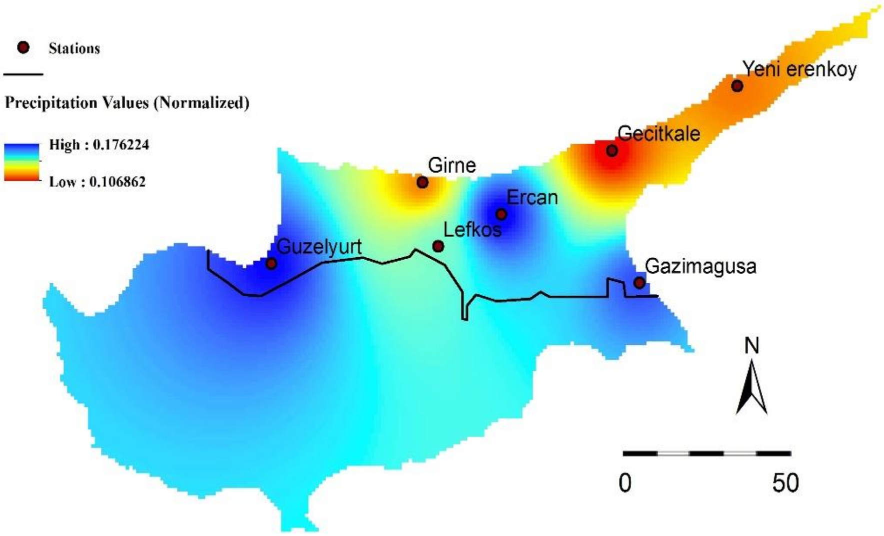

(c) Spatial precipitation distribution for annual average-2015.

Figure 4.6: Spatial precipitation distribution for different time spans.

4.3 Comparative Analysis of the Methods

For instance, the obtained results of spatiotemporal modelling for Ercan and Girne stations are depicted in Figure 4.7 and 4.8, respectively.

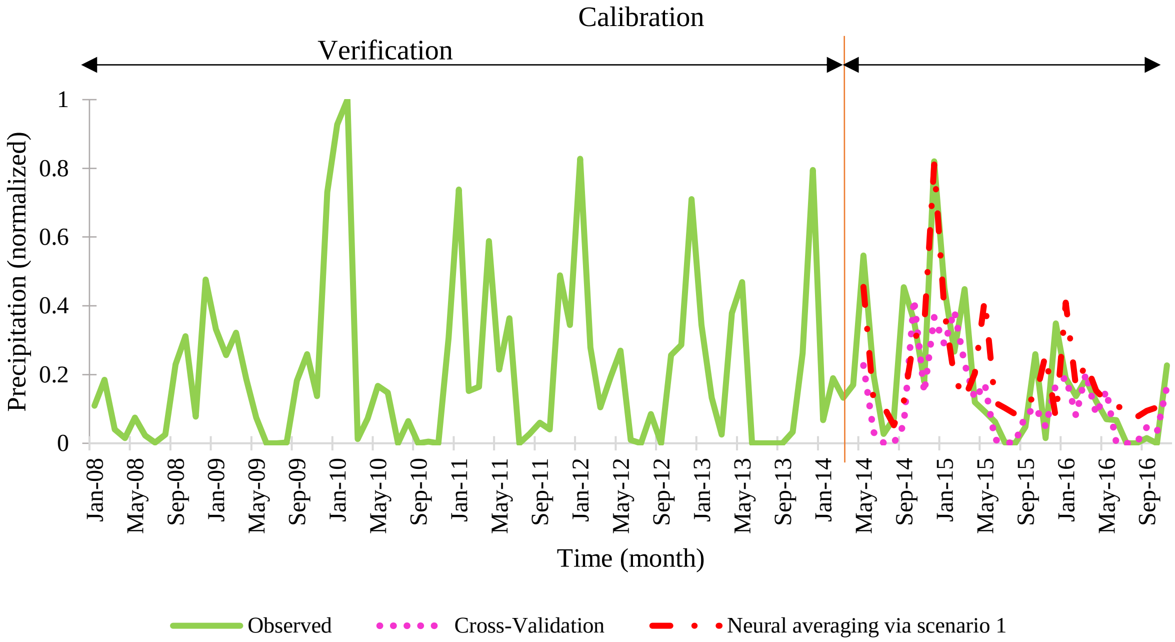

(a) Observed versus estimated precipitation by IDW model

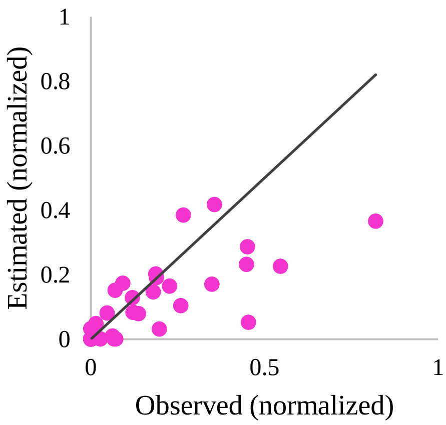

(b) Scatter plot for verification period

Figure 4.7: Results of cross-validation method for Ercan station **(a)** Observed versus estimated precipitation by IDW model. **(b)** Scatter plot for verification period

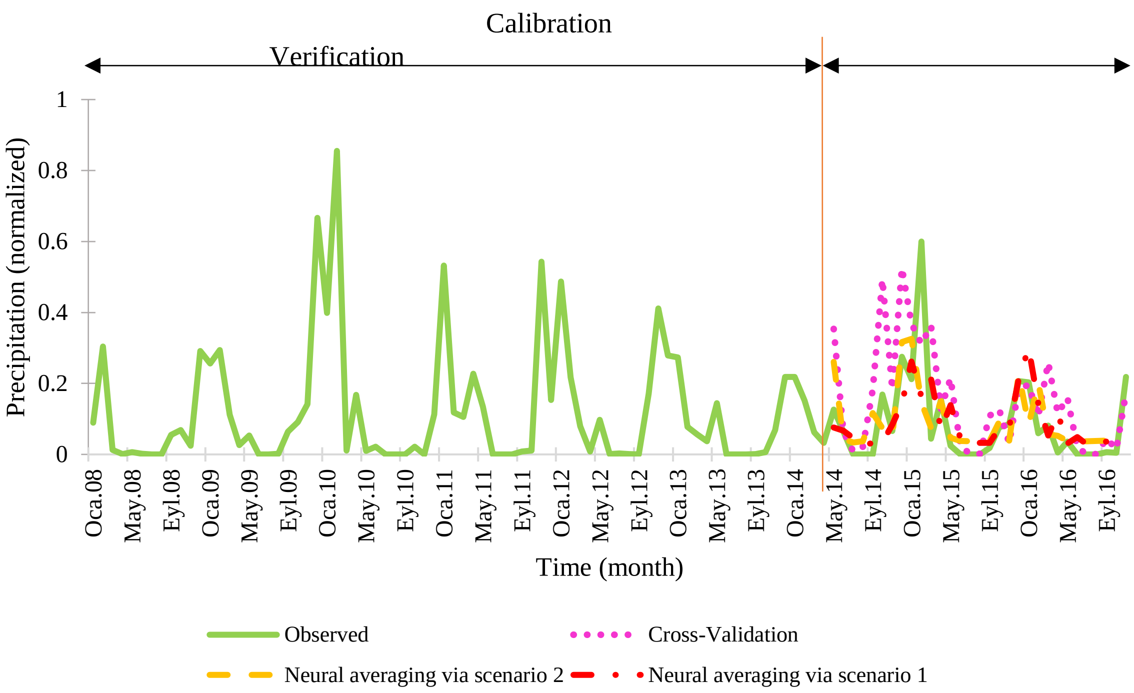

(a) Observed versus estimated precipitation by IDW model

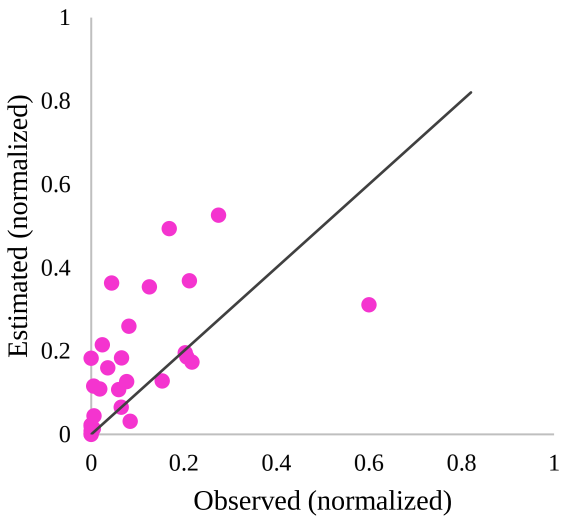

(b) Scatter plot for verification period

Figure 4.8: Results of cross-validation method for Girne station **(a)** Observed versus estimated precipitation by IDW model. **(b)** Scatter plot for verification period

As it's clear from Figures 4.7 and 4.8, almost in most cases the IDW method had better and more accurate results in dry seasons than in flood seasons. It denotes that the data obtained during dry seasons are more regular than in flood seasons. This point of view in this study is consistent with the study done by Kong and Tong, (2008). It would be therefore considered that spatial pattern of rainfall in flood season is inferior to the data interpolated during dry seasons due to extreme rainfall events. Also Chen and Liu, (2012) proved that rainfall data interpolation using IDW can obtain more accurate results during the dry season than in the flood season.

The overall results of the study however show that the proposed two-stage spatiotemporal precipitation modeling by employing unique tools in both time and space modeling stages, could lead to appropriate outcomes. These results are applicable for practical usages, since both temporal and spatial models demonstrate desired values and features at each time step.

CHAPTER 5
CONCLUSIONS

In this thesis, for spatiotemporal modeling of precipitation over North Cyprus, a two-stage hybrid modeling was provided. In this way, firstly the FFNN, ANFIS and LSSVM predictors were developed using the precipitation data from seven different stations installed in different locations of TRNC. Thereafter, the ensemble methods were employed to increase the temporal modeling efficiency. Secondly, the outputs of neural ensemble method (as the best temporal modeling tool) were utilized in the spatial modeling stage. In this stage, through seven steps for all stations, one station's data were individually removed from the modeling process and then, it's values were estimated by the predicted values from six other stations for the verification period.

At temporal stage two scenarios were considered with different input variables that in scenario 1 each station's own pervious data was used for modeling while in scenario 2, the central station's (Ercan station) data were also employed in addition to each station's own data. The results of two employed scenarios indicated that scenario 2 had better performance and could enhance the modeling efficiency up to 58%, in the verification step because of employing the observed data from the Ercan station as exogenous input in simulating other stations' precipitation. Whereas, among three single AI models, the FFNN model provided better performance in most cases in the verification step. Analysis of the results in terms of computed DC and RMSE values showed that the ensemble methods provide better results with regard to the single AI based methods. Furthermore, the ensemble model based on the non-linear neural averaging produced better predictions than the single models and linear ensemble models up to 38% and 54% for calibration and verification steps, respectively.

The IDW interpolation method was employed for the spatial estimation of precipitation. The cross-validation results showed that the model is able to produce successful estimations for monthly precipitation values over the region with average DC value of 0.7. Furthermore, IDW method was more beneficial than AI methods in cases that a station's own data contains some degrees of noises.

Limitations and Future Research

One of the limitations of the considered temporal ensembling method is related with the continuously averaging the outputs of the simple AI models. For future increasing the performance of the temporal modelling will be challenging the development of the adaptive sampling method for dynamically selection the outputs of single AI-based models in terms of the minimum error approximation.

For the larger study area having more scattered spatial observation points (stations), stochastic spatial interpolation methods (e.g., Kriging) may be used instead of IDW method which needs only a few data points. Also in this case due to the correlation between precipitation and ground level of stations, a multivariate analysis (such as Co-Kriging) may be used to enhance the accuracy of the spatial interpolation results considering the elevation of the station as the secondary interpolation parameter.

REFERENCES

Abbot, J., and Marohasy, J. (2012). *Application of Artificial Neural Networks to Rainfall Forecasting in Queensland, Australia*. Advances in Atmospheric Sciences, 29(4), 717 –730.

Adeloye, A. J., and Montaseri, M. (2002). *Preliminary Stream Flow Data Analyses Prior to Water Resources Planning Study*. Journal of Hydrological Sciences. 47, 679 – 692.

Akrami, S. A., Nourani, V., and Hakim, S. J. S. (2014). *Development of Nonlinear Model Based on Wavelet-ANFIS for Rainfall Forecasting at Klang Gates Dam*. Water Resources Management, 28(10), 2999 – 3018.

Alexandersson, H. (1986). *A Homogeneity Test Applied to Precipitation Data.* Journal of Climatology, 6, 661 – 675.

Alpers, W., and Melsheimer, C. (2004). *Rainfall.* SAR Marine User Manual, US Department of Commerce, NOAA.

American Meteorological Society (2009) *Rainfall.* Glossary of Meteorology, Archived From the Original on 2008-10-09. Retrieved 2009-01-02.

ASCE Task Committee on Application of Artificial Neural Networks in Hydrology (2000). *Artificial Neural Networks in Hydrology. II: Hydrologic applications.* Journal of Hydrologic Engineering, 5(2), 124 - 137.

Ashraf, M., Loftis, J. C., and Hubbard, K. G. (1997*). Application of Geostatistics to Evaluate Partial Weather Station Networks.* Agricultural and Forest Meteorology, 84, 255 – 271.

Bates, J. M., and Granger, C. W. J. (1969). *The Combination of Forecasts*. Operations Research Quarterly, 20, 451 – 468.

Bisht, D., Joshi, M. C., and Mehta, A. (2015). *Prediction of Monthly Rainfall of Nainital Region Using Artificial Neural Network and Support Vector Machine*. International Journal of Advance Research and Innovative Ideas in Education, 1(3), 2395 - 4396.

Brown, M., and C. Harris,. (1994). *Neurofuzzy Adaptive Modelling and Control*. Prentice-Hall, Englewood Cliffs, New Jersey.

Burrough, P. A. (1986). *Principles of Geographic Information Systems for Land Resource Assessment*. Monographs on Soil and Resources Survey No.12, Oxford Science Publications, New York.

Buishand, T. A. (1982). *Some methods for testing the homogeneity of rainfall records*. Journal of Hydrology, 58, 11 – 27.

Caruso, C., and Quarta, F. (1998). *Interpolation Methods Comparison.* Computers and Mathematics with Applications, 35(12), 109 – 126.

Chen, F. W., and Liu, C. W. (2012). *Estimation of the spatial rainfall distribution using inverse distance weighting (IDW) in the middle of Taiwan*. Paddy and Water Environment, 10(3), 209 - 222.

Cortes, C., and Vapnik, V. (1995). *Support Vector Networks*. Machine Learning, 20(3), 273 - 297.

Danandeh M. A., Nourani, V., Karimi K. V., and Ghorbani, M. A. (2018). *A Hybrid Support Vector Regression–Firefly Model For Monthly Rainfall Forecasting*. International Journal of Environmental Science and Technology, 1-12. https://rd.springer.com/article/10.1007/s13762-018-1674-2 (accessed 15 January 2019)

Devi, S. R., Arulmozhivarman, P., and Venkatesh, C. (2017). *ANN Based Rainfall Prediction - A Tool for Developing a Landslide Early Warning System*. Advancing Culture of Living with Landslides- Workshop on World Landslide Forum, 175-182.

Franke R., and Nielson G. M. (1991). *Scattered Data Interpolation and Applications: A Tutorial and Survey, in Geometric Modelling: Methods and Their Applications,* H. Hagen & D. Roller (eds.), Springer, 1990, pp. 131-160.

Govindaraju, R. S. (2000). *Artificial Neural Networks in Hydrology. I: Preliminary concepts.* Journal of Hydrologic Engineering, 5(2), 115-123.

Granata, F., Papirio, S., Esposito, G., Gargano, R., and Marinis, G. (2017). *Machine Learning Algorithms For The Forecasting Of Wastewater Quality Indicators*. Water, 9(2), 105.

Guhathakurta, P. (2008). *Long Lead Monsoon Rainfall Prediction for Meteorological Sub-Divisions of India Using Deterministic Artificial Neural Network Model*. Meteorology and Atmospheric Physics, 101(2), 93–108.

Hagan, M. T., and Menhaj, M. B. (1996). *Training Feed Forward Networks with Marquardt Algorithm.* IEEE Trans Neural Network, 5, 989-92.

Hung, N. Q., Babel, M. S., Weesakul, S., and Tripathi, N. K. (2009). *An Artificial Neural Network Model for Rainfall Forecasting in Bangkok, Thailand*. Hydrology and Earth System Sciences, 13, 1413-1425.

Isaaks, E. H., and Srivastava, R. M. (1989). *An Introduction to Applied Geostatistics*. Oxford University Press, New York.

Jang, J. S. R., Sun, C. T., and Mizutani, E. (1997). *Neuro-Fuzzy And Soft Computing; A Computational Approach To Learning And Machine Intelligence*. Prentice-Hall, New Jersey.

Kasiviswanathan, K. S., Cibin, R., Sudheer, K. P., and Chaubey, I. (2013). *Constructing Prediction Interval For Artificial Neural Network Rainfall Runoff Models Based On Ensemble Simulations.* Journal of Hydrology, 499, 275-288.

Keskin, M. E., Taylan D., and Terzi O. (2006). *Adaptive Neural-Based Fuzzy Inference System (ANFIS) Approach For Modelling Hydrological Time Series.* Hydrological Sciences, (51)4, 588-598.

Khalili, N., Khodashenas, S. R., Davary, K., Mousavi, B., and Karimaldini, F. (2016). *Prediction of Rainfall Using Artificial Neural Networks For Synoptic Station Of Mashhad: A Case Study.* Arabian Journal Of Geosciences, 9(624).

Kisi, O., and Cimen, M. (2012). *Precipitation Forecasting By Using Wavelet-Support Vector Machine Conjunction Model.* Engineering Applications Of Artificial Intelligence, 25(4), 783-792.

Kong, Y. F., and Tong, W. W. (2008). *Spatial Exploration And Interpolation Of The Surface Precipitation Data.* Geographical Research, 27(5), 1097–1108.

Kourentzes, N., Barrow, D. K., and Crone, F. (2014). *Neural Network Ensemble Operators For Time Series Forecasting.* Expert Systems with Applications, 41, 4235-4244.

Legates, D. R., and McCabeJr, G.J. (1999). *Evaluating the Use of Goodness-Of-Fit Measures In Hydrologic And Hydroclimatic Model Validation*. Water Resources Research, 35(1), 233–241.

Lu, K., and Wang, L. (2011). *A Novel Nonlinear Combination Model Based On Support Vector Machine For Rainfall Prediction.* In: Fourth International Joint Conference On Computational Sciences and Optimization (CSO), Fourth International Joint Conference. IEEE. 1343–1347.

Lu, G. Y., and Wong, D. W. (2008). *An Adaptive Inverse-Distance Weighting Spatial Interpolation Technique*. Computational Geosciences, 34(9), 1044–1055.

Makridakis, S., Andersen, A., Carbone, R., Fildes, R., Hibon, M., Lewandowski, R., and Winkler, R. (1982*). The Accuracy Of Extrapolation (Time Series) Methods: Results Of A Forecasting Competition*. Journal of Forecasting, 1(2), 111-153.

Mehdizadeh, S., Behmanesh, J., and Khalili, K. (2018). *New Approaches For Estimation Of Monthly Rainfall Based On GEP-ARCH And ANN-ARCH Hybrid Models.* Water Resources Management, 32(2), 527-45.

Moore, D.S. (1987). *In Chi-square tests, in Studies in Statistics, Mathematical Association of America;* R.V. Hogg, R.V., Ed.; Washington D.C., USA, vol. 19, pp. 66–106.

Nourani, V., and Andalib, G. (2015). *Daily and Monthly Suspended Sediment Load Predictions Using Wavelet-Based AI Approaches.* Journal of Mountain Science, 12(1), 85-100.

Nourani, V., Ejlali, R. G., and Alami, M. T. (2010). *Spatiotemporal Groundwater Level Forecasting In Coastal Aquifers By Hybrid Artificial Neural Network-Geostatisics Model: A Case Study*. Environmental Engineering Science, 28(3), 217–228.

Nourani, V., Komasi, M., and Mano, A. (2009). *A Multivariate ANN-Wavelet Approach for Rainfall–Runoff Modeling.* Water Resources Management, 23(14), 2877–2894.

Nourani, V., and Komasi, M. (2013). *A Geomorphology-Based ANFIS Model For Multi-Station Modelling Of Rainfall–Runoff Process.* Journal of Hydrology (490), 41-55.

Nourani, V., and Parhizkar, M. (2013). *Conjunction of SOM-Based Feature Extraction Method And Hybrid Wavelet-ANN Approach For Rainfall–Runoff Modelling.* Journal of Hydroinformatics 15(3), 829-848.

Nourani, V., RezapourKhanghah, T., and Hosseini Baghanam, A. (2014). *Implication of Feature Extraction Methods to Improve Performance of Hybrid Wavelet-ANN Rainfall–Runoff Model. In: Case Studies in Intelligent Computing*, Issac, B., Israr, N. (Eds.), Taylor and Francis Group, New York, 457–498.

Nourani, V., Sharghi, E., and Aminfar, M. H. (2012). *Integrated ANN Model For Earthfilldams Seepage Analysis: Sattarkhan Dam In Iran.* Artificial Intelligence Research 1(2), 22-37.

Parmar, K. S., and Bhardwaj, R. (2015). *River Water Prediction Modeling Using Neural Networks, Fuzzy And Wavelet Coupled Model*. Water Resources Management, 29(1), 17-33.

Partal, T., and Cigizoglu, H. K. (2008). *Estimation and Forecasting of Daily Suspended Sediment Data Using Wavelet-Neural Networks*. Journal of Hydrology, 358(3–4), 317–331.

Pettitt, A. N. (1979). *A Non-Parametric Approach to the Change-Point Problem.* Appl. Stat., 28, 126–135.

Price, C., Michaelides, S., Pashiardis, S., and Alperta, P. (1999). *Long Term Changes In Diurnal Temperature Range In Cyprus.* Atmospheric Research, 51(2), 85–98.

Rajaee, T., Mirbagheri, S. A., Nourani, V., and Alikhani, A. (2009a*). Prediction of Daily Suspended Sediment Load Using Wavelet And Neuro-Fuzzy Combined Model.* Journal of Environmental Science and Technology, 7, 93-110.

Rizzo, D. M., and Dougherty, D. E. (1994). *Characterization of Aquifer Properties Using Artificial Neural Networks: Neural Kriging*. Water Resources Research, 30, 483–497.

Sahoo, M., Das, T., Kumari, K., and Dhar, A. (2017). *Space–time Forecasting Of Groundwater Level Using A Hybrid Soft Computing Model.* Hydrological Sciences Journal, 62(4), 561-574.

Shahidi, M., and Abedini, M. J. (2018). *Optimal Selection Of Number And Location Of Rain Gauge Stations For Areal Estimation Of Annual Rainfall Using A Procedure Based On Inverse Distance Weighting Estimator.* Paddy and Water Environment, 16(3), 617-629.

Sharghi, E., Nourani, V., and Behfar, N. (2018). *Earthfill Dam Seepage Analysis Using Ensemble Artificial Intelligence Based Modeling.* Journal of Hydroinformatics, 20(5), 1071-1084.

Sharifi, S. S., Delirhasannia, R., Nourani, V., Sadraddini, A. A., and Ghorbani, A. (2013). *Using ANNs and ANFIS for Modeling And Sensitivity Analysis Of Effective Rainfall*. Recent Advances in Continuum Mechanics, Hydrology and Ecology, 133-139.

Singh, V. K., Kumar, P., Singh, B. P., and Malik, A. (2016). *A Comparative Study Of Adaptive Neuro Fuzzy Inference System (ANFIS) And Multiple Linear Regression*

(MLR) For Rainfall-Runoff Modeling. International Journal of Science and Nature, **7**(4), 714-723.

Sojitra, M. A., Purohit, R. C., and Pandya, P. A. (2015). *Comparative Study Of Daily Rainfall Forecasting Models Using Anfis*. Current World Environment, 10(2), 529-536.

Souto, Y. M., Porto, F., Moura, A. M., and Bezerra E. (2018*). A Spatiotemporal Ensemble Approach to Rainfall Forecasting.* International Joint Conference on Neural Networks (IJCNN).

Steinskog, D.J., Tjostheim, D.B., and Kvamsto, N.G. (2007). *A Cautionary Note On The Use Of The Kolmogorov–Smirnov Test For Normality*. Mon. Weather Rev., *135*, 1151–1157.

Theodossiou, N., and Latinopoulos, P. (2006). *Evaluation and Optimisation Of Groundwater Observation Networks Using The Kriging Methodology*. Environmental Modeling and Software, 21(7), 991–1000.

Vaheddoost, B., and Aksoy, H. (2017). *Structural Characteristics Of Annual Precipitation In Lake Urmia Basin.* Theor. Appl. Climatol., 128, 919–932.

Yamashkin, S., Radovanovic, M., Yamashkin, A., and Vukovic, D. (2018). *Using Ensemble Systems To Study Natural Processes.* Journal Of Hydroinformatics, 20(4), 753-765.

Yang, H. H., Vuuren, S. V., Sharma, S., and Hermansky, H. (2000). *Relevance of Time Frequency Features For Phonetic And Speaker-Channel Classification*. Speech Communication, 31,35-50.

Yaseen, Z .M., Ghareb, M. I., Ebtehaj, I., Bonakdari, H., Siddique, R., Heddam, S., Yusif, A. A., and Deo, R. (2018). *Rainfall Pattern Forecasting Using Novel Hybrid Intelligent Model Based ANFIS-FFA.* Water Resources Management, 32(1), 105-122.

Zhang, G. P., and Berardi V. L. (2001). *Time Series Forecasting With Neural Network Ensembles: An Application For Exchange Rate Prediction*. Journal of the Operational Research Society, 52, 652-664.

Zhang, G. P. (2003). *Time Series Forecasting Using A Hybrid ARIMA And Neural Network Model.* Neurocomputing, 50, 159-175.

APPENDICES

APPENDIX-1

MATLAB CODES

Appendix 1.1: MATLAB Codes for FFNN

```
clc
clear all
it1=input('input data :');
data=xlsread(it1);
Output =data(:,end);
Input=data(:,1:end-1);
a=numel(Output);
a=round(a*0.75);
it=Input(1:a,:);
tt = Output(1:a);
iv=Input(a+1:end,:);
tv = Output(a+1:end);
it=it';
tt=tt';
iv=iv';
tv=tv';
maxHn=input('max Hn :');
maxEpoch=input('max Epoch :');
ot=cell(maxHn,maxEpoch/10);
ov=cell(maxHn,maxEpoch/10);
RMSEtrain=cell(maxHn,maxEpoch/10);
RMSEverification=cell(maxHn,maxEpoch/10);
DCtrain=cell(maxHn,maxEpoch/10);
DCverification=cell(maxHn,maxEpoch/10);
TR=cell(maxHn,maxEpoch/10);
```

```
NET=cell(maxHn,maxEpoch/10);
for epoch=10:10:maxEpoch
for Hn=1:maxHn
net=newff(it,tt,Hn,{'tansig' 'tansig'},'trainlm');
net=init(net);
net.divideFcn='';
net.trainParam.epochs=epoch;
net.trainParam.show=NaN;
[net,tr,ot{Hn,epoch/10}]=train(net,it,tt);
NET{Hn,epoch/10}=net;
TR{Hn,epoch/10}=tr;
ov{Hn,epoch/10}=sim(net,iv);
RMSEtrain{Hn,epoch/10}=sqrt(mean((ot{Hn,epoch/10}-tt).^2,2));
RMSEverification{Hn,epoch/10}=sqrt(mean((ov{Hn,epoch/10}-tv).^2,2));
DCtrain{Hn,epoch/10}=1-RMSEtrain{Hn,epoch/10}.^2./var(tt,1,2);
DCverification{Hn,epoch/10}=1-RMSEverification{Hn,epoch/10}.^2./var(tv,1,2);
end
end
xlswrite('DCtrain.xls',DCtrain);
xlswrite('DC verify.xls',DCverification);
xlswrite('RMSEtrain.xls',RMSEtrain);
xlswrite('RMSEverification.xls',RMSEverification);
```

Appendix 1.2: MATLAB Codes for ANFIS

```
clear all
clc
close all;
inputtrain=xlsread('anfistest',1,'a:d');
outputtrain=xlsread('anfistest',1,'e:e');
inputtest=xlsread('anfistest',2,'a:d');
outputtest=xlsread('anfistest',2,'e:e');
trnData=xlsread('anfistest',1,'a:e');
testData=xlsread('anfistest',2,'a:e');
%%
%ANFIS    ANFIS       ANFIS         ANFIS        ANFIS
%% Design Fis (Training Data)
% fismat=genfis1(trnData,numMFs,inmftype,outmftype);
for training_epoch_number=5:50:500   %10:50:300       %$$$$$$$$$$$$$$$$$$$$$$
for iMF=2:4   %2:4                                   %%$$$$$$$$$$$$$$$$$$$$$
numMFs=iMF;
for iTYPE=1:8   %1:8        %$$$$$$$$$$$$$$$$$$$$$$
if iTYPE==1
inmftype='gaussmf';
end
if iTYPE==2
inmftype='trimf';
end
if iTYPE==3
inmftype='gbellmf';
end
if iTYPE==4
inmftype='trapmf';
end
if iTYPE==5
```

```
inmftype='gauss2mf';
end
if iTYPE==6
inmftype='pimf';
end
if iTYPE==7
inmftype='dsigmf';
end
if iTYPE==8
inmftype='psigmf';
end
% % if iTYPE==9
% %     inmftype='smf';
% % end
outmftype='linear';
fismat=genfis1(trnData,numMFs,inmftype,outmftype);
% fismat=anfis(trnData,initFis,trnOpt,dispOpt,chkData,optMethod)
initFis=fismat;
%training_epoch_number=100;
training_error_goal=0;
initial_step_size=0.01;
step_size_decrease_rate=0.9;
step_size_increase_rate=1.1;
trnOpt=[training_epoch_number...
training_error_goal...
initial_step_size...
step_size_decrease_rate...
step_size_increase_rate];
ANFIS_information=false;
error_opt=false;
step_size_opt=false;
```

```
final_results_opt=true;
dispOpt=[ANFIS_information...
error_opt...
step_size_opt...
final_results_opt];
chkData=[];
optMethod=0;  % 1=hybrid , 0=backpr
fismat=anfis(trnData,initFis,trnOpt,dispOpt,chkData,optMethod);
%% GENFIS3
% %fismat = genfis3(Xin,Xout,type,cluster_n,fcmoptions)
% Xin=inputtrain;
% Xout=outputtrain;
% type='sugeno';
% cluster_n='auto';
% fismat = genfis3(Xin,Xout,type,cluster_n);
%% GENFIS2
%% Apply ANFIS to Train Data
outputtrain_ANFIS=evalfis(inputtrain,fismat);
trnError=outputtrain-outputtrain_ANFIS;
trnMSE=mean(trnError.^2);
trnRMSE=sqrt(trnMSE);
%DC
r111=(outputtrain-mean(outputtrain));
r111=sum(r111.^2);
trnDC=1-sum(trnError.^2)/r111;
%% Apply ANFIS to Test Data
outputtest_ANFIS=evalfis(inputtest,fismat);
testError=outputtest-outputtest_ANFIS;
testMSE=mean(testError.^2);
testRMSE=sqrt(testMSE);
%DC
```

```
r222=(outputtest-mean(outputtest));
r222=sum(r222.^2);
testDC=1-sum(testError.^2)/r222;
if trnDC>0.4&testDC>0.4
fprintf('\n\nEpoch=%i TRAIN
MF=%i\t%s\tRMSE=%f\tDC=%f',training_epoch_number,iMF,inmftype,trnRMSE,trnDC)
;
fprintf('\nEpoch=%i TEST
MF=%i\t%s\tRMSE=%f\tDC=%f',training_epoch_number,iMF,inmftype,testRMSE,testD
C);
end
end %end of ITYPE
end  %end of NMF
end
```

Appendix 1.3: MATLAB Codes for LSSVM

```
clc
clear all
it1=input('input data :');
data=xlsread(it1);
%%
Output=data(:,end);
Input=data(:,1:end-1);
a=numel(Output);
a=round(a*0.75);
train.inp=Input(1:a,:);
train.out=Output(1:a);
test.inp=Input(a+1:end,:);
test.out=Output(a+1:end);
%model = initlssvm(X,Y,'function',gam,sig2,'RBF_kernel');
X=train.inp;
Y=train.out;
cd 'LSSVMlabv'
%param
[gam,sig2]=tunelssvm({X,Y,'function',[],[],'RBF_kernel'},'simplex','crossvalidatelssvm',{5,
'mse'});
%[gam,sig2] =
tunelssvm({X,Y,'classification',[],[],'RBF_kernel'},'simplex','crossvalidatelssvm',{5,'miscla
ss'});
%  Number_of_selected_Instance=size(train,1)
model={X,Y,'function',gam,sig2,'RBF_kernel'};
% Train SVR
model=trainlssvm(model);
% Prediction Section
Yp(i)=simlssvm(model, X);
cd '..'
```

```
%% test
% Prediction Section
cd 'LSSVMlabv'
Yp(i)=simlssvm(model, test.inp);
cd '..'
[r2 rmse]=rsquare(test.out,Yp)
disp(['rmse : ' num2str(rmse)]);
```

APPENDIX-2:

FRAGMENT OF DAILY DATA FROM METEOROLOGICAL STATION OF THE TURKISH REPUBLIC OF NORTHERN CYPRUS FOR 2016

To prevent using the data without the permission of the author, below are given data covering only 1 year (2016) for all stations.

2016 DAILY PRECIPITATION AMOUNT FOR *GIRNE* STATION (mm)													
DAY	JAN	FEB	MAR	APR	MAY	JUNE	JULY	AUG	SEP	OCT	NOV	DEC	YEARLY
1	6.5	0.0	0.0	0.0	0.0	0.0	0.0	0.0	0.0	0.0	25.6	33.2	65.3
2	0.0	0.0	0.0	0.0	0.0	0.0	0.0	0.0	0.0	0.0	0.0	8.4	8.4
3	0.0	0.0	0.4	0.0	0.0	0.0	0.0	0.0	1.0	0.0	0.0	0.0	1.4
4	20.2	0.0	0.4	0.0	0.8	0.0	0.0	0.0	0.0	0.0	0.00	0.0	21.4
5	1.8	0.6	1.2	0.0	2.2	0.0	0.0	0.0	0.0	0.0	0.0	0.0	5.8
6	0.0	2.2	0.0	0.0	1.2	0.0	0.0	0.0	0.0	0.0	0.0	0.0	3.4
7	4.2	0.0	0.0	0.0	7.8	0.0	0.0	0.0	0.0	0.0	0.0	0.0	12.0
8	1.3	0.0	0.0	0.0	0.0	0.0	0.0	0.0	0.0	0.0	0.0	0.0	1.3
9	0.0	0.0	0.0	0.0	0.0	0.0	0.0	0.0	0.0	0.0	0.0	0.0	0.0
10	0.0	5.8	0.0	0.0	0.0	0.0	0.0	0.0	0.0	0.0	0.0	0.0	5.8
11	0.7	2.5	0.0	1.2	0.0	0.0	0.0	0.0	0.0	0.0	0.0	0.0	4.4
12	0.1	0.0	0.0	0.6	0.0	0.0	0.0	0.00	0.0	0.0	0.0	0.2	0.9
13	0.0	0.0	0.0	0.0	0.0	0.0	0.0	0.0	0.0	0.0	0.0	35.0	35.0
14	0.0	0.0	5.2	0.0	0.0	0.0	0.0	0.0	0.0	0.0	0.0	5.2	10.4
15	0.0	0.0	10.2	0.0	0.0	0.0	0.0	0.0	0.0	0.0	0.0	0.0	10.2
16	0.0	0.0	4.2	0.0	0.0	0.0	0.0	0.0	0.0	0.0	0.0	1.8	6.0
17	0.0	0.0	0.0	0.0	0.0	0.0	0.0	0.0	0.0	0.0	0.0	5.0	5.0
18	3.8	0.0	0.0	0.0	0.0	0.0	0.0	0.0	0.0	1.6	0.0	0.8	6.2
19	6.2	0.0	0.0	0.0	0.0	0.0	0.0	0.0	0.0	0.0	0.0	0.0	6.2
20	0.2	0.0	0.0	0.0	0.0	0.0	0.0	0.0	0.0	0.0	0.0	0.0	0.2
21	1.2	7.6	0.0	0.0	0.0	0.0	0.0	0.0	1.0	0.0	0.0	23.0	32.8
22	3.2	0.0	0.0	0.0	0.0	0.0	0.0	0.0	0.0	0.0	0.0	56.4	59.6
23	15.6	0.0	0.0	0.0	0.0	0.0	0.0	0.0	0.0	0.0	0.0	3.0	18.6
24	2.8	0.0	0.0	0.0	0.0	0.0	0.0	0.0	0.0	0.0	0.0	124.0	126.8
25	0.0	0.0	0.0	0.0	0.0	0.0	0.0	0.0	0.0	0.0	0.0	17.6	17.6
26	0.0	0.0	0.0	0.0	0.0	0.0	0.0	0.0	0.0	0.0	0.0	1.4	1.4
27	0.0	0.0	0.0	0.0	0.0	0.0	0.0	0.0	0.0	0.0	0.0	5.0	5.0
28	0.0	0.0	5.6	0.0	0.0	0.0	0.0	0.0	0.00	0.0	0.0	0.2	5.8
29	0.0	0.0	0.0	0.0	0.0	0.0	0.0	0.0	0.0	0.0	8.6	10.4	19.0
30	0.0		0.0	0.0	0.0	0.0	0.0	0.0	0.0	0.0	36.2	2.6	38.8
31	0.0		0.0		0.0		0.0	0.0		0.0		1.0	1.0
TOTAL	67.8	18.7	27.2	1.8	12.0	0.0	0.0	0.0	2.0	1.6	70.4	334.2	535.7

2016 DAILY PRECIPITATION AMOUNT FOR *GUZELYURT* STATION (mm)													
DAY	**JAN**	**FEB**	**MAR**	**APR**	**MAY**	**JUNE**	**JULY**	**AUG**	**SEP**	**OCT**	**NOV**	**DEC**	**YEARLY**
1	11.4	0.0	0.0	0.0	0.0	0.0	0.0	0.0	0.0	0.0	13.1	25.2	**49.7**
2	0.0	0.0	0.0	0.0	0.0	0.0	0.0	0.0	0.0	0.0	0.0	2.2	**2.2**
3	0.0	0.0	0.3	0.0	0.0	0.0	0.0	0.0	0.0	0.0	0.0	0.0	**0.3**
4	10.8	0.0	0.5	0.0	1.6	0.0	0.0	0.0	0.6	0.0	0.0	0.0	**13.5**
5	0.3	1.3	0.7	0.0	2.8	0.1	0.0	0.0	0.0	0.0	0.0	0.0	**5.2**
6	0.0	4.4	0.0	0.0	2.6	0.0	0.0	0.0	0.0	0.0	0.0	0.0	**7.0**
7	5.0	0.1	0.0	0.0	0.1	0.0	0.0	0.0	0.0	0.0	0.0	0.3	**5.5**
8	0.0	0.0	0.0	0.0	0.1	0.0	0.0	0.0	0.0	0.0	0.0	0.0	**0.1**
9	0.0	0.0	0.0	0.0	0.0	0.0	0.0	0.0	0.0	0.0	0.0	0.0	**0.0**
10	0.0	1.5	0.0	0.0	0.0	0.0	0.0	0.0	0.0	0.0	0.0	0.0	**1.5**
11	0.9	0.0	0.0	0.0	0.0	0.0	0.0	0.0	0.0	0.0	0.0	0.0	**0.9**
12	0.0	0.0	0.0	1.7	0.0	0.0	0.0	0.0	0.0	0.0	0.0	3.4	**5.1**
13	0.2	0.0	0.0	0.0	0.0	0.0	0.0	0.0	0.0	0.0	0.0	9.9	**10.1**
14	0.3	0.0	2.2	0.0	0.0	0.0	0.0	0.0	0.0	0.0	0.0	0.8	**3.3**
15	0.0	0.0	17.7	0.0	0.0	0.0	0.0	0.0	0.0	0.0	0.0	0.0	**17.7**
16	0.0	0.0	0.0	0.0	0.1	0.0	0.0	0.0	0.0	0.0	0.0	0.5	**0.6**
17	0.0	0.0	0.0	0.0	0.0	0.0	0.0	0.0	0.0	0.0	0.0	10.4	**10.4**
18	10.1	0.0	0.0	0.0	0.0	0.0	0.0	0.0	0.0	0.0	0.0	1.2	**11.3**
19	1.7	0.0	0.0	0.0	0.0	0.0	0.0	0.0	0.0	0.0	0.0	0.0	**1.7**
20	0.0	0.0	0.0	0.0	0.0	0.0	0.0	0.0	0.0	0.0	0.0	0.0	**0.0**
21	1.2	4.9	0.0	0.0	0.0	0.0	0.0	0.0	1.3	0.0	0.0	5.6	**13.0**
22	0.0	0.1	0.0	0.0	0.0	0.0	0.0	0.0	0.0	0.0	0.0	7.2	**7.3**
23	0.0	0.0	0.0	0.0	0.0	0.0	0.0	0.0	19.6	0.0	0.0	0.0	**19.6**
24	6.8	0.0	0.0	0.0	0.0	0.0	0.0	0.0	0.0	0.0	0.0	1.5	**8.3**
25	0.0	0.0	0.0	0.0	0.0	0.0	0.0	0.0	0.0	0.0	0.0	15.1	**15.1**
26	0.0	0.0	0.0	0.0	0.0	0.0	0.0	0.0	0.0	0.0	0.0	0.7	**0.7**
27	0.0	0.0	0.0	0.0	0.0	0.0	0.0	0.0	0.0	0.0	0.0	0.1	**0.1**
28	0.0	0.0	2.4	0.0	0.0	0.0	0.0	0.0	0.0	0.0	0.0	0.1	**2.5**
29	0.0	0.0	0.0	0.0	0.0	0.0	0.0	0.0	0.0	0.0	6.8	5.8	**12.6**
30	0.0		0.0	0.0	0.0	0.0	0.0	0.0	0.0	0.0	35.1	5.9	**41.0**
31	0.0		0.0		0.0		0.0	0.0		0.0		0.7	**0.7**
TOTAL	**48.7**	**12.3**	**23.8**	**1.7**	**7.3**	**0.1**	**0.0**	**0.0**	**21.5**	**0.0**	**55.0**	**96.6**	**267.0**

2016 DAILY PRECIPITATION AMOUNT FOR *LEFKOŞA* STATION (mm)													
DAY	**JAN**	**FEB**	**MAR**	**APR**	**MAY**	**JUNE**	**JULY**	**AUG**	**SEP**	**OCT**	**NOV**	**DEC**	**YEARLY**
1	0.0	0.2	0.0	0.0	0.0	0.0	0.0	0.0	0.0	0.0	1.4	37.4	**39.0**
2	0.0	0.0	0.0	0.0	0.0	0.0	0.0	0.0	0.0	0.0	0.2	4.0	**4.2**
3	0.0	0.0	0.0	0.0	0.0	0.0	0.0	0.0	4.8	0.0	0.0	0.0	**4.8**
4	9.2	0.0	1.0	0.0	1.0	0.0	0.0	0.0	0.0	0.0	0.00	0.0	**11.2**
5	2.0	1.2	0.8	0.0	3.2	0.0	0.0	0.0	0.0	0.0	0.0	0.2	**7.4**
6	0.2	1.8	0.0	0.0	0.6	0.0	0.0	0.0	0.0	0.0	0.0	0.0	**2.6**
7	2.4	0.0	0.0	0.0	16.4	0.0	0.0	0.0	0.0	0.0	0.0	0.0	**18.8**
8	0.4	0.0	0.0	0.0	0.2	0.0	0.0	0.0	0.0	0.0	0.0	0.0	**0.6**
9	0.0	0.0	0.0	0.2	0.0	0.0	0.0	0.0	0.0	0.0	0.0	0.0	**0.2**
10	0.0	0.0	0.0	0.0	0.0	0.0	0.0	0.0	0.0	0.0	0.0	0.0	**0.0**
11	0.6	0.0	0.0	1.6	0.0	0.0	0.0	0.0	0.0	0.0	0.0	0.0	**2.2**
12	0.0	0.0	0.0	15.6	0.0	0.0	0.0	0.0	0.0	0.0	0.0	0.6	**16.2**
13	0.2	0.2	0.0	0.0	0.0	0.0	0.0	0.0	0.0	0.0	0.0	10.0	**10.4**
14	0.6	0.0	16.4	0.0	0.0	0.0	0.0	0.0	0.0	0.0	0.0	0.4	**17.4**
15	0.0	0.0	15.4	0.0	0.0	0.0	0.0	0.0	0.0	0.0	0.0	0.0	**15.4**
16	0.0	0.0	10.8	0.0	0.0	0.0	0.0	0.0	0.0	0.0	0.0	0.0	**10.8**
17	0.2	0.0	0.0	0.0	0.0	0.0	0.0	0.0	0.0	0.0	0.0	5.4	**5.6**
18	4.8	0.0	0.0	0.0	0.0	0.0	0.0	0.0	0.0	0.2	0.0	1.2	**6.2**
19	2.4	0.0	0.0	0.0	0.0	0.0	0.0	0.0	0.0	0.0	0.0	0.0	**2.4**
20	0.0	0.0	0.0	0.0	0.0	0.0	0.0	0.0	0.0	0.0	0.0	0.0	**0.0**
21	1.4	10.2	0.0	0.0	0.0	0.0	0.0	0.0	0.2	0.0	0.0	7.6	**19.4**
22	0.4	0.0	0.0	0.0	0.0	0.0	0.0	0.0	0.2	0.0	0.0	12.6	**13.2**
23	1.0	0.0	0.0	0.0	0.0	0.0	0.0	0.0	0.0	0.0	0.0	3.0	**4.0**
24	0.4	0.0	0.0	0.0	0.0	0.0	0.0	0.0	0.0	0.0	0.0	0.4	**0.8**
25	0.0	0.0	0.0	0.0	0.0	0.0	0.0	0.0	0.0	0.0	0.0	9.4	**9.4**
26	0.0	0.0	0.0	0.0	0.0	0.0	0.0	0.0	0.0	0.0	0.0	1.4	**1.4**
27	0.0	0.0	0.0	0.0	8.4	0.0	0.0	0.0	0.0	0.0	0.0	0.4	**8.8**
28	0.0	0.0	3.0	0.0	0.2	0.0	0.0	0.0	0.00	0.0	0.0	0.2	**3.4**
29	0.0	0.0	0.0	0.0	0.0	0.0	0.0	0.0	0.0	0.0	6.6	10.8	**17.4**
30	0.0		0.0	0.0	0.0	0.0	0.0	0.0	0.0	0.0	8.6	5.0	**13.6**
31	0.0		0.0		0.0		0.0	0.0		0.0		0.6	**0.6**
TOTAL	**26.2**	**13.6**	**47.4**	**17.4**	**30.0**	**0.0**	**0.0**	**0.0**	**5.2**	**0.2**	**16.8**	**110.6**	**267.4**

2016 DAILY PRECIPITATION AMOUNT FOR *ERCAN* STATION (mm)													
DAY	**JAN**	**FEB**	**MAR**	**APR**	**MAY**	**JUNE**	**JULY**	**AUG**	**SEP**	**OCT**	**NOV**	**DEC**	**YEARLY**
1	0.1	0.0	0.0	0.0	0.0	0.0	0.0	0.0	0.0	0.0	10.3	19.9	**30.3**
2	0.0	0.0	0.0	0.0	0.0	0.0	0.0	0.0	0.0	0.0	0.0	1.1	**1.1**
3	0.0	0.0	0.1	0.0	0.0	0.0	0.0	0.0	0.0	0.0	0.0	0.0	**0.1**
4	3.6	0.0	2.0	0.0	0.1	0.0	0.0	0.0	0.1	0.0	0.0	0.0	**5.8**
5	0.0	0.6	0.3	0.0	2.5	0.0	0.0	0.0	0.4	0.0	0.0	0.0	**3.8**
6	0.0	11.6	0.0	0.0	0.0	0.0	0.0	0.0	0.4	0.0	0.0	0.0	**12.0**
7	7.8	0.0	0.0	0.0	3.1	0.0	0.0	0.0	0.0	0.0	0.0	0.0	**10.9**
8	0.5	0.0	0.0	0.0	0.0	0.0	0.0	0.0	0.0	0.0	0.0	0.0	**0.5**
9	0.0	0.0	0.0	0.0	0.0	0.0	0.0	0.0	0.0	0.0	0.0	0.0	**0.0**
10	0.6	0.2	0.0	0.0	0.0	6.1	0.0	0.0	0.0	0.0	0.0	0.0	**6.9**
11	0.0	0.1	0.0	0.5	0.0	1.0	0.0	0.0	0.0	0.0	0.0	0.0	**1.6**
12	0.0	0.0	0.0	14.3	0.0	0.0	0.0	0.0	0.0	0.0	0.0	0.3	**14.6**
13	0.0	0.1	0.0	0.0	0.0	0.0	0.0	0.0	0.0	0.0	0.0	9.3	**9.4**
14	0.0	0.0	11.9	0.0	0.0	0.0	0.0	0.0	0.0	0.0	0.0	0.1	**12.0**
15	0.0	0.0	4.8	0.0	0.0	0.0	0.0	0.0	0.0	0.0	0.0	0.0	**4.8**
16	0.0	0.0	3.0	0.0	0.0	0.0	0.0	0.0	0.0	0.0	0.0	0.0	**3.0**
17	8.0	0.0	0.0	0.0	0.0	0.0	0.0	0.0	0.0	0.0	0.0	2.1	**10.1**
18	1.8	0.0	0.0	0.0	0.0	0.0	0.0	0.0	0.0	0.0	0.0	0.6	**2.4**
19	0.0	0.0	0.0	0.0	0.0	0.0	0.0	0.0	0.0	0.0	0.0	0.0	**0.0**
20	0.3	0.0	0.0	0.0	0.0	0.0	0.0	0.0	0.0	0.0	0.0	0.0	**0.3**
21	0.7	3.4	0.0	0.0	0.0	0.0	0.0	0.0	0.7	0.0	0.0	19.4	**24.2**
22	0.1	0.0	0.0	0.0	0.0	0.0	0.0	0.0	0.0	0.0	0.0	23.6	**23.7**
23	0.0	0.0	0.0	0.0	0.0	0.0	0.0	0.0	0.2	0.0	0.0	3.2	**3.4**
24	0.0	0.0	0.0	0.0	0.0	0.0	0.0	0.0	0.0	0.0	0.0	4.4	**4.4**
25	0.0	0.0	0.0	0.0	0.0	0.9	0.0	0.0	0.0	0.0	0.0	4.6	**5.5**
26	0.0	0.0	0.0	0.0	0.0	0.0	0.0	0.0	0.0	0.0	0.0	1.1	**1.1**
27	0.0	0.0	0.0	0.0	2.7	0.0	0.0	0.0	0.0	0.0	0.0	1.3	**4.0**
28	0.0	0.0	1.2	0.0	0.2	0.0	0.0	0.0	0.0	0.0	0.0	0.0	**1.4**
29	0.0	0.0	0.0	0.0	0.0	0.0	0.0	0.0	0.0	0.0	4.0	10.0	**14.0**
30	0.0		0.0	0.0	0.0	0.0	0.0	0.0	0.0	0.0	13.1	9.9	**23.0**
31	0.0		0.0		0.0		0.0	0.0		0.0		0.5	**0.5**
TOTAL	**23.5**	**16.0**	**23.3**	**14.8**	**8.6**	**8.0**	**0.0**	**0.0**	**1.8**	**0.0**	**27.4**	**111.4**	**234.8**

2016 DAILY PRECIPITATION AMOUNT FOR *GEÇİTKALE* STATION (mm)													
DAY	**JAN**	**FEB**	**MAR**	**APR**	**MAY**	**JUNE**	**JULY**	**AUG**	**SEP**	**OCT**	**NOV**	**DEC**	**YEARLY**
1	0.0	0.8	0.0	0.0	0.0	0.0	0.0	0.0	0.0	0.0	6.4	16.6	**23.8**
2	0.0	0.2	0.0	0.0	0.0	0.0	0.0	0.0	0.0	0.0	0.0	2.2	**2.4**
3	0.0	0.0	0.0	0.0	0.0	0.0	0.0	0.0	0.0	0.0	0.0	0.0	**0.0**
4	2.2	0.0	0.4	0.0	0.0	0.0	0.0	0.0	0.0	0.0	0.0	0.0	**2.6**
5	0.8	0.0	0.6	0.0	3.2	0.0	0.0	0.0	0.0	0.0	0.0	0.6	**5.2**
6	0.4	6.2	0.0	0.0	0.2	0.0	0.0	0.0	28.6	0.0	0.0	0.0	**35.4**
7	0.2	0.0	0.0	0.0	23.6	0.0	0.0	0.0	0.0	0.0	0.0	0.4	**24.2**
8	1.0	0.0	0.0	0.0	0.0	0.0	0.0	0.0	0.0	0.0	0.0	0.0	**1.0**
9	0.2	0.0	0.0	0.0	0.0	0.0	0.0	0.0	0.0	0.0	0.0	0.0	**0.2**
10	0.0	0.2	0.0	0.0	0.0	0.0	0.0	0.0	0.0	0.0	0.0	0.0	**0.2**
11	0.0	0.0	0.0	2.4	0.0	0.0	0.0	0.0	0.0	0.0	0.0	0.0	**2.4**
12	0.2	0.0	0.0	16.4	0.0	0.0	0.0	0.0	0.0	0.0	0.0	0.2	**16.8**
13	0.0	0.0	0.0	0.0	0.0	0.0	0.0	0.0	0.0	0.0	0.0	5.6	**5.6**
14	0.0	0.0	10.4	0.0	0.0	0.0	0.0	0.0	0.0	0.0	0.0	5.4	**15.8**
15	0.0	0.0	3.6	0.0	8.4	0.0	0.0	0.0	0.0	0.0	0.0	0.0	**12.0**
16	0.0	0.0	1.0	0.0	0.0	0.0	0.0	0.0	0.0	0.0	0.0	0.0	**1.0**
17	0.0	0.0	0.0	0.0	0.0	0.0	0.0	0.0	0.0	0.0	0.0	3.4	**3.4**
18	9.2	0.0	0.0	0.0	0.0	0.0	0.0	0.0	0.0	32.6	0.0	1.0	**42.8**
19	7.0	0.0	0.0	0.0	0.0	0.0	0.0	0.0	0.0	0.0	0.0	0.0	**7.0**
20	0.0	0.0	0.0	0.0	0.0	0.0	0.0	0.0	0.0	0.0	0.0	0.0	**0.0**
21	0.0	1.4	0.0	0.0	0.0	0.0	0.0	0.0	0.2	0.0	0.0	6.8	**8.4**
22	7.0	2.6	0.0	0.0	0.0	0.0	0.0	0.0	0.0	0.0	0.0	15.8	**25.4**
23	0.2	0.0	0.0	0.0	0.0	0.0	0.0	0.0	0.0	0.0	0.0	28.4	**28.6**
24	0.0	0.0	0.0	0.0	0.0	0.0	0.0	0.0	0.0	0.0	0.0	0.2	**0.2**
25	0.0	0.0	0.0	0.0	0.0	0.0	0.0	0.0	0.0	0.0	0.0	17.0	**17.0**
26	0.0	0.0	0.0	0.0	0.0	0.0	0.0	0.0	0.0	0.0	0.0	2.2	**2.2**
27	0.0	0.0	0.0	0.0	15.0	0.0	0.0	0.0	0.0	0.0	0.0	0.6	**15.6**
28	0.0	0.0	1.2	0.0	0.2	0.0	0.0	0.0	0.0	0.0	0.0	0.0	**1.4**
29	0.0	0.0	0.0	0.0	0.0	0.0	0.0	2.0	0.0	0.0	2.6	19.4	**24.0**
30	0.0		0.0	0.0	0.0	0.0	0.0	0.0	0.0	0.0	6.0	18.6	**24.6**
31	0.2		0.0		0.0		0.0	0.0		1.2		1.2	**2.6**
TOTAL	**28.6**	**11.4**	**17.2**	**18.8**	**50.6**	**0.0**	**0.0**	**2.0**	**28.8**	**33.8**	**15.0**	**145.6**	**351.8**

2016 DAILY PRECIPITATION AMOUNT FOR *GAZİMAĞUSA* STATION (mm)													
DAY	**JAN**	**FEB**	**MAR**	**APR**	**MAY**	**JUNE**	**JULY**	**AUG**	**SEP**	**OCT**	**NOV**	**DEC**	**YEARLY**
1	0.0	0.2	0.0	0.0	0.0	0.0	0.0	0.0	0.0	0.0	30.1	12.7	**43.0**
2	0.0	0.0	0.0	0.0	0.0	0.0	0.0	0.0	0.0	0.0	0.0	0.6	**0.6**
3	0.0	0.0	0.4	0.0	0.0	0.0	0.0	0.0	0.0	0.0	0.0	0.0	**0.4**
4	10.0	0.0	10.0	0.0	0.0	0.0	0.0	0.0	0.0	0.0	0.0	0.0	**20.0**
5	0.4	1.0	1.8	0.0	1.4	0.0	0.0	0.0	0.0	0.0	0.0	0.2	**4.8**
6	0.0	3.8	0.0	0.0	2.3	0.0	0.0	0.0	0.0	0.0	0.0	0.0	**6.1**
7	6.3	0.0	0.0	0.0	6.4	0.0	0.0	0.0	0.0	0.0	0.0	0.0	**12.7**
8	0.0	0.0	0.0	0.0	0.1	0.0	0.0	0.0	0.0	0.0	0.0	0.0	**0.1**
9	0.0	0.0	0.0	0.0	0.0	2.0	0.0	0.0	0.0	0.0	0.0	0.0	**2.0**
10	0.0	0.0	0.0	0.0	0.0	0.0	0.0	0.0	0.0	0.0	0.0	0.0	**0.0**
11	0.8	0.0	0.0	0.2	0.0	0.0	0.0	0.0	0.0	0.0	0.0	0.0	**1.0**
12	0.0	0.0	0.0	12.1	0.0	0.0	0.0	0.0	0.0	0.0	0.0	0.9	**13.0**
13	0.0	0.0	0.0	11.2	0.0	0.0	0.0	0.0	0.0	0.0	0.0	5.3	**16.5**
14	0.0	0.0	6.7	0.0	0.0	0.0	0.0	0.0	0.0	0.0	0.0	3.9	**10.6**
15	0.0	0.0	3.2	0.0	0.0	0.0	0.0	0.0	0.0	0.0	0.0	0.0	**3.2**
16	0.0	0.0	0.2	0.0	0.4	0.0	0.0	0.0	0.0	0.0	0.0	0.0	**0.6**
17	0.0	0.0	0.0	0.0	0.0	0.0	0.0	0.0	0.0	0.0	0.0	1.9	**1.9**
18	7.1	0.0	0.0	0.0	0.0	0.0	0.0	0.0	0.0	9.8	0.0	0.8	**17.7**
19	0.0	0.0	0.0	0.0	0.0	0.0	0.0	0.0	0.0	0.0	0.0	0.0	**0.0**
20	0.0	0.0	0.0	0.0	0.0	0.0	0.0	0.0	0.4	0.0	0.0	0.0	**0.4**
21	0.0	1.7	0.0	0.0	0.0	0.0	0.0	0.0	0.8	0.0	0.0	8.9	**11.4**
22	0.0	1.6	0.0	0.0	0.0	0.0	0.0	0.0	0.0	0.0	0.0	23.9	**25.5**
23	5.4	0.0	0.0	0.0	1.3	0.0	0.0	0.0	0.0	0.0	0.0	5.2	**11.9**
24	0.0	0.0	0.0	0.0	0.0	0.0	0.0	0.0	0.0	0.0	0.0	2.1	**2.1**
25	0.0	0.0	0.0	0.0	0.0	0.0	0.0	0.0	0.0	0.0	0.0	3.0	**3.0**
26	0.0	0.0	0.0	0.0	0.0	0.0	0.0	0.0	0.0	0.0	0.0	4.7	**4.7**
27	0.0	0.0	0.0	0.0	0.6	0.0	0.0	0.0	0.0	0.0	0.0	0.0	**0.6**
28	0.0	0.0	0.0	0.0	3.5	0.0	0.0	0.0	0.0	0.2	0.0	0.0	**3.7**
29	0.0	0.0	0.0	0.0	0.0	0.0	0.0	0.0	0.0	0.0	1.0	11.9	**12.9**
30	0.0		0.0	0.1	0.0	0.0	0.0	0.0	0.0	0.0	5.7	15.8	**21.6**
31	0.4		0.0		0.0		0.0	0.0		0.0		0.5	**0.9**
TOTAL	**30.4**	**8.3**	**22.3**	**23.6**	**16.0**	**2.0**	**0.0**	**0.0**	**1.2**	**10.0**	**36.8**	**102.3**	**252.9**

2016 DAILY PRECIPITATION AMOUNT FOR *YENİERENKÖY* STATION(mm)													
DAY	**JAN**	**FEB**	**MAR**	**APR**	**MAY**	**JUNE**	**JULY**	**AUG**	**SEP**	**OCT**	**NOV**	**DEC**	**YEARLY**
1	0.0	0.0	0.0	0.0	0.0	0.0	0.0	0.0	0.0	0.0	33.2	18.6	**51.8**
2	0.0	0.0	0.0	0.0	0.0	0.0	0.0	0.0	0.0	0.0	0.2	1.0	**1.2**
3	0.0	0.0	2.4	0.0	0.0	0.0	0.0	0.0	0.0	0.0	0.0	0.6	**3.0**
4	8.4	0.0	5.8	0.0	8.8	0.0	0.0	0.0	0.0	0.0	0.0	2.2	**25.2**
5	0.0	0.4	0.2	0.0	16.2	0.0	0.0	0.0	1.4	0.0	0.0	0.0	**18.2**
6	0.0	10.4	0.0	0.0	0.6	0.0	0.0	0.0	0.0	0.0	0.0	0.0	**11.0**
7	3.2	0.0	0.0	0.0	0.8	0.0	0.0	0.0	0.0	0.0	0.0	0.0	**4.0**
8	12.2	0.0	0.0	0.0	0.0	0.0	0.0	0.0	0.0	0.0	0.0	0.0	**12.2**
9	0.0	0.0	0.0	0.0	0.0	0.0	0.0	0.0	0.0	0.0	0.0	0.0	**0.0**
10	0.0	0.0	0.0	0.0	0.0	0.0	0.0	0.0	0.0	0.0	0.0	0.0	**0.0**
11	1.2	0.0	0.0	0.0	0.0	0.0	0.0	0.0	0.0	0.0	0.0	0.0	**1.2**
12	0.0	0.0	0.0	1.0	0.0	0.0	0.0	0.0	0.0	0.0	0.0	0.0	**1.0**
13	0.2	0.0	0.0	3.6	0.0	0.0	0.0	0.0	0.0	0.0	0.0	11.6	**15.4**
14	0.0	0.0	24.4	0.0	0.0	0.0	0.0	0.0	0.0	0.0	0.0	6.8	**31.2**
15	0.0	0.0	8.4	0.0	0.0	0.0	0.0	0.0	0.0	0.0	0.0	0.0	**8.4**
16	0.0	0.0	6.8	0.0	0.0	0.0	0.0	0.0	0.0	0.0	0.0	3.0	**9.8**
17	0.0	0.0	0.0	0.0	0.0	0.0	0.0	0.0	0.0	0.0	0.0	1.4	**1.4**
18	8.6	0.0	0.0	0.0	0.0	0.0	0.0	0.0	0.0	1.2	0.0	0.6	**10.4**
19	1.2	0.0	0.0	0.0	0.0	0.0	0.0	0.0	0.0	0.0	0.0	0.0	**1.2**
20	0.0	0.0	0.0	0.0	0.0	0.0	0.0	0.0	0.2	0.0	0.0	0.0	**0.2**
21	0.0	1.4	0.0	0.0	0.0	0.0	0.0	0.0	0.4	0.0	0.0	8.6	**10.4**
22	3.8	6.0	0.0	0.0	0.0	0.0	0.0	0.0	0.0	0.0	0.0	25.8	**35.6**
23	6.8	0.0	0.0	0.0	0.8	0.0	0.0	0.0	0.0	0.0	0.0	11.8	**19.4**
24	2.2	0.0	0.0	0.0	0.0	0.0	0.0	0.0	0.0	0.0	0.0	18.2	**20.4**
25	2.2	0.0	0.0	0.0	0.0	0.0	0.0	0.0	0.0	0.0	0.0	16.8	**19.0**
26	0.6	0.0	0.0	0.0	0.0	0.0	0.0	0.0	0.0	0.0	0.0	2.0	**2.6**
27	0.0	0.0	4.0	0.0	0.0	0.0	0.0	0.0	0.0	0.0	0.0	6.2	**10.2**
28	0.0	0.0	6.4	0.0	0.0	0.0	0.0	0.0	0.0	0.0	0.0	1.6	**8.0**
29	0.0	0.0	0.0	0.0	0.0	0.0	0.0	0.0	0.0	0.0	3.2	20.0	**23.2**
30	1.0		0.0	0.0	0.0	0.0	0.0	0.0	0.0	0.0	16.6	15.0	**32.6**
31	0.0		0.0		0.0		0.0	0.0		0.0		5.2	**5.2**
TOTAL	**51.6**	**18.2**	**58.4**	**4.6**	**27.2**	**0.0**	**0.0**	**0.0**	**2.0**	**1.2**	**53.2**	**177.0**	**393.4**

CURRICULUM VITAE

Name: **Selin ÜZELALTINBULAT**

Date of Birth: **22/07/1987**

Degree	Field	Institution	Date
B. Sc.	Computer Information Systems	Near East University	2006-2011
M. Sc.	Computer Engineering	Near East University	2011-2013
Ph. D.	Computer Engineering	Near East University	2014- 2019

1. Publications:

1.1. *International Journals:*

1.1.1. Nourani, V., **Uzelaltinbulat, S.,** Sadikoglu, F., Behfar N. Artificial Intelligence Based Ensemble Modeling for Multi-Station Prediction of Precipitation, *Atmosphere*, 2019, 10:2. (SCI-E)

1.1.2. **Uzelaltinbulat, S.**, Sadikoglu, F., Nourani, V. Comparative Analysis of Artificial Intelligence Based Methods for Prediction of Precipitation. Case Study: North Cyprus, Book Series in *Advances in Intelligent Systems and Computing,* 2018, volume 896, 51-64. (SCOPUS)

1.1.3. **Uzelaltinbulat, S.,** Ugur, B. Lung tumor segmentation algorithm, *Procedia Computer Science,* 2017, Volume 120, 140-144. (SCOPUS)

1.1.4. Musayev, A., **Uzelaltinbulat, S.,** Mammadova, S., Gardashova, L., Musayeva, A. Estimation of impact of the changes made to the tax legislation to the tax receipts through fuzzy numbers, *Procedia Computer Science*, 2017, Volume 120, 333-340. (SCOPUS)

1.1.5. Sadikoglu, F., **Uzelaltinbulat, S.** Biometric Retina Identification Based on Neural Network, *Procedia Computer Science*, 2016, Volume 102, 26-33. (SCOPUS)

1.2. International Presentations and Proceedings :

1.2.1. **Uzelaltinbulat, S.**, Sadikoglu, F., Nourani, V. Comparative Analysis of Artificial Intelligence Based Methods for Prediction of Precipitation. Case Study: North Cyprus, Book Series in *Advances in Intelligent Systems and Computing,* International Conference on Theory and Applications of Fuzzy Systems and Soft Computing, ICAFS 2018, Poland, 27-28 August, volume 896, 51-64. (WEB OF SCIENCE)

1.2.2. **Uzelaltinbulat, S.,** Ugur, B. "*Lung tumor segmentation algorithm*" The Nineth International Conference on Theory and Application of Soft Computing, Computing with Words and Perception (ICSCCW-2017) 22-23 August, Budapest, Hungary. (WEB OF SCIENCE)

1.2.3. Musayev, A., **Uzelaltinbulat, S.,** Mammadova, S., Gardashova, L., Musayeva, A. "*Estimation of impact of the changes made to the tax legislation to the tax receipts through fuzzy numbers*" The Nineth International Conference on Theory and Application of Soft Computing, Computing with Words and Perception (ICSCCW-2017) 22-23 August, Budapest, Hungary. (WEB OF SCIENCE)

1.2.4. Sadikoglu, F., **Uzelaltinbulat, S.** "*Biometric Retina Identification Based on Neural Network*". Twelfth International Conference on Application of Fuzzy Systems and Soft Computing (ICAFS-2016) 29-30 August, Vienna, Austria. (WEB OF SCIENCE)

2. Academic/Administrative Duties:

2.1. Vice Restor Assistant (2012- present)

2.2. Lecturer of Engineering Faculty, Department of Computer Engineering, Near East University (2013-present)

2.3. Lecturer of Engineering Faculty, Department of Maritime Studies and Maritime Management&Administration, University of Kyrenia (2016-2017 Academic Year)

3. **Citations:**

3.1. Google Scholar:

https://scholar.google.com.tr/citations?user=o-1xTloAAAAJ&hl=tr

4. **Scientific, Organizational and Professional Duties:**

4.1. Organization Committee Member of ICSCCW 2019 (International Conference of Theory and Application of Soft Computing, Computing with Words and Perception), Prague, Czech Republic, 2019.

http://www.icsccw2019.com

4.2. Organization Committee Member of ICAFS 2018 (International Conference of Application of Fuzzy Logic and Soft Computing), Warsaw, Poland, 2018. http://www.icafs2018.com/

4.3. Organization Committee Member of ICSCCW 2017 (International Conference of Theory and Application of Soft Computing, Computing with Words and Perception), Budapest, Hungary, 2017.

http://www.icsccw2017.com

4.4. Organization Committee Member of ICAFS 2016 (International Conference of Application of Fuzzy Logic and Soft Computing), Vienna, Austria, 2016.

http://www.icafs-2016.com/

5. **Courses Taught During the Years:**

Academic Year	**Semester**	**Course Code**	**Weekly Hours**		**Number of Students**
			Theory	**Lab**	
2013-2014	Fall	BİL 131, BİL 132, BLG 141 BLG 142, BİL 101	2	2	142
	Spring				88
2014-2015	Fall	BİL 131, BİL 132, BLG 141 BLG 142, BİL 101	2	2	151
	Spring				73
2015-2016	Fall	BİL 131, BİL 132, BLG 141 BLG 142, BİL 101	2	2	126
	Spring				37

2016-2017	Fall	BİL 131, BİL 132, BLG 141 BLG 142, BİL 101	2	2	98
	Spring				78
2017-2018	Fall	MOD 101	2	2	85
	Spring	MOD 101, MOD 106, CEIT 208			50
2018-2019	Fall	MOD 101, MOD 106	2	2	71
	Spring	MOD 101			30

6. Sertificates:

6.1. Certificate of "Eğiticinin Eğitimi" given by Near East University Rectorate, 2017.

7. Awards:

7.1. *Best Paper Award*, 13th International Conference on Application of Fuzzy Systems and Soft Computing, ICAFS 2018, Warsaw, Poland, 27-28 August 2018.

7.2. Near East University Academician Awards Ceremony 2018, *Best Paper Award*, given from ICAFS 2018 Conference.

7.3. Near East University Academician Awards Ceremony 2017, *Young Academician Award*, given by Near East University Rectorate.

7.4. 2010-2011 Academic Year Fall Semester *Honour Certificate* at Department of Computer Information Systems, Near East University.

7.5. 2009-2010 Academic Year Spring Term *Honour Certificate* at Department of Computer Information Systems, Near East University.

7.6. 2007-2008 Academic Year Fall Term *Honour Certificate* at Department of Computer Information Systems, Near East University.